

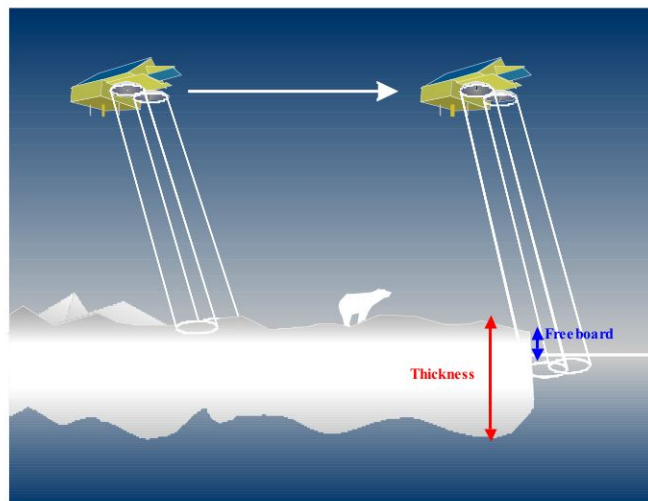
Nansen Environmental and Remote Sensing Center



NERSC Technical Report no. 257

PRODEX Kontrakt no. C90149



CryoSat pre-launch cal- val studies of sea ice thickness



Authors:

*Stein Sandven, Kjell Kloster, Hanne Sagen and Vitaly Alexandrov
(Nansen Environmental and Remote Sensing Center)
Sebastian Gerland and Richard Hall (Norwegian Polar Institute)
Rene Forsberg and Sine Munk Hvidegaard (Danish National Space Center)
Christian Haas (Alfred Wegener Institute)*

September 2005

 <p>Nansen Environmental and Remote Sensing Center (NERSC) Thormøhlensgate 47 N-5006 Bergen, Norway Phone: + 47 55 20 58 00 Fax: + 47 55 20 58 01 E-Mail: Stein.Sandven@nersc.no http://www.nersc.no</p>	 <p>Norwegian Polar Institute (NPI) Polar Environmental Centre N-9296 Tromsø, Norway Phone: + 47 77 75 05 00 Fax: + 47 55 75 05 01 E-mail: sebastian.gerland@npolar.no http://npweb.npolar.no</p>
--	--

<p>TITLE: CryoSat pre-launch calibration and validation studies of sea ice thickness</p>	<p>REPORT IDENTIFICATION NERSC Technical report no. 257</p>
<p>CLIENT ESA PRODEX</p>	<p>CONTRACT Contract Number: C90149</p>
<p>CLIENT REFERENCE Mr. B. Zufferey</p>	<p>AVAILABILITY Open</p>
<p>INVESTIGATORS Stein Sandven, NERSC Kjell Kloster, NERSC Hanne Sagen, NERSC Vitaly Alexandrov, NERSC Sebastian Gerland, NPI Richard Hall, NPI Rene Forsberg, DNSC Sine Munk Hvidegaard, DNSC Christian Haas, AWI</p>	<p>AUTHORISATION Bergen, 30 September 2005 Ola M. Johannessen</p>

Contents

EXECUTIVE SUMMARY.....	2
1.1 THE FIELD EXPERIMENT IN MARCH – APRIL 2003	3
1.2 PHYSICAL FOUNDATION: ISOSTATIC EQUILIBRIUM OF ICE FLOATING ON WATER	5
1.3 BASIC CONCEPTS OF CRYOSAT SEA ICE THICKNESS RETRIEVAL.....	5
1.4 ERROR ESTIMATES.....	6
2. AIRCRAFT DATA	8
3. ICE THICKNESS MEASUREMENTS USING HELICOPTER AND IN SITU TECHNIQUES.....	11
3.1 GROUND-BASED PROFILING USING AN EM31 THICKNESS SENSOR	12
3.2 SIMS (SEA ICE MONITORING SYSTEM): CONTINUOUS ALONG-TRACK ICE THICKNESS MEASUREMENTS	12
3.3 AIRBORNE THICKNESS PROFILING USING AN EM BIRD	15
3.4 GROUND PENETRATING RADAR.....	17
3.5 RESULTS FROM THE BARENTS SEA AND STORFJORDEN.....	18
3.6 LASER PROFILING OF PRESSURE RIDGES.....	21
4. IN SITU MEASUREMENTS OF SEA ICE AND SNOW PARAMETERS.....	22
4.1 ICE CORING BY AWL.....	22
4.2 SNOW MEASUREMENTS BY NERSC.....	24
5. PROCESSING OF D2P LEVEL 1B DATA OVER SEA ICE.....	26
5.1 BACKGROUND	26
5.2 RADAR ALTIMETER SIGNAL.....	26
5.3 PROCESSING OF WAVEFORMS.....	27
5.4 RANGE CALIBRATION AND HEIGHT OF SIGNAL.....	27
5.5 PROCESSING TO ALONG-TRACK PROFILES.....	28
5.6 DISCUSSION.....	29
6. SYNTHESIS OF RESULTS	31
6.1 COMPARISONS ON 11 APRIL.....	31
6.2 COMPARISONS ON 15 APRIL.....	33
6.3 CALCULATION AND DIRECT MEASUREMENT OF ICE THICKNESS	34
6.4 ICE THICKNESS SYNTHESIS MAPS FROM AIRBORNE AND SATELLITE LASER DATA	36
7. RESULTS OF PRE-LAUNCH SEA ICE CAL/VAL ACTIVITIES AT NORWEGIAN POLAR INSTITUTE	38
7.1 OVERVIEW.....	38
7.2 IN SITU MEASUREMENT TECHNIQUES	39
7.3 SELECTED RESULTS.....	39
7.4 FROM FREEBOARD/DRAFT TO ICE THICKNESS	41
7.5 OUTLOOK	42
8. CONCLUDING REMARKS AND PLANS FOR FURTHER WORK	43
9. REFERENCES.....	44

Executive Summary

This study gives an overview of CryoSat pre-launch cal-val experiments for sea ice thickness studies performed in the Fram Strait and Svalbard area in 2003 and 2004. The experiments described in the report include:

- March 2003: Polarstern conducted field measurements and helicopter surveys in the Barents Sea – Storfjorden area
- April 2003: The CryoVax cal-val campaign was conducted in the area north of Svalbard using Twin Otter aircraft with D2P radar, scanning laser and GPS measurements. Scientists on Polarstern with helicopter and in situ field measurements were participating.
- September 2003 and 2004: Lance conducted in situ sea ice measurements in the Fram Strait at about 79 N during summer conditions when there was little sea ice in the area.

In situ measurements of snow and ice properties were obtained by drilling holes and using ground penetrating radar. The most intensive collection of in situ measurements were obtained in the area around Polarstern during its 10 day drift phase from 7 to 17 April. This drift phase was coordinated with the CryoVex aircraft surveys in the same area. The most important parameters were snow thickness, ice thickness including ridges, temperature, salinity and density of the ice.

Helicopter profiles of surface height and ice thickness were obtained using electromagnetic induction (EM-profiles). Use of helicopter EM-profiling has become a well-established technique for measuring ice thickness on local and regional scale. In CryoVex, this was the main method to compare with the aircraft surveys where long profiles of freeboard and thickness were obtained both with laser and radar altimeter. The EM-method itself was also validated on local scale by in situ drilling and ground penetrating radar.

A Twin Otter aircraft equipped with scanning laser, video, GPS and a D2P radar altimeter conducted a series of flights over sea ice in the Fram Strait area and north of Greenland. The scanning laser in combination with GPS gives accurate profiles of the snow surface. These profiles, which were obtained during relative cloud-free periods, are used to estimate freeboard of snow plus ice. The D2P radar altimeter (Delayed Doppler Phase monopulse), which is similar to the radar altimeter onboard CryoSat, provided profiles of freeboard of the sea ice surface, assuming that the radar signal in Ku-band (13.9 Ghz) is reflected at the snow-ice interface. Two 100 km long tracks of simultaneous helicopter and aircraft surveys were conducted starting from the position of Polarstern. The freeboard data and derived thickness from the two parallel surveys were inter-compared, and both data sets were compared with the in situ measurements.

Satellite data, in particular Synthetic Aperture Radar (SAR) images were obtained and used to map ice types, leads, floes and ice drift. By collocating ice type information from SAR with freeboard and thickness profiles from laser and D2P radar, the signals from the two altimeter systems can be studied in relation to ice properties observed in the SAR images. A large part of the data collected during the experiments have not yet been analyzed. The results of the analysis so far indicate that different observing systems are in general agreement, but further work is needed to understand how the radar altimeter signal interacts with the snow and ice. The scanning laser showed capability to measure freeboard to an accuracy of about 0.05 m, and the D2P is expected to be similar. To invert freeboard to thickness has additional errors due to the uncertainty in the ice density which can vary from 830 kgm⁻³ to 915 kgm⁻³.

The first extensive pre-launch validation data for CryoSat is presently analyzed and new results will soon be published. With launch of CryoSat in October 2005, it will be necessary to follow up the cal-val work with post-launch experiments from 2006 and onwards. The International Polar Year will offer good opportunities for such work in the coming 2 – 3 years.

1. Introduction

1.1 The field experiment in March – April 2003

This report describes the main results of the CryoSat pre-launch experiment for sea ice, which was carried out by an international team during the period March – April 2003 in the Barents Sea and Fram Strait area. One of the main objectives of CryoSat is to retrieve sea ice thickness from radar altimetry in the Arctic for climate monitoring. The validation of the thickness retrieval from altimeter data is a key activity to determine the accuracy of the radar measurements and to assess the performance of the method in different parts of the Arctic. In this study, use of different observing techniques for sea ice thickness and related parameters is demonstrated and some results are presented and discussed. The data obtained for the experiments were used to measure ice surface height, ice draft, freeboard of snow and ice surface and physical properties of snow and ice which determine the density of sea ice. The different observing techniques are summarized in Table 1.

The experiment was carried out in two phases using R/V Polarstern as the main platform. The first phase took place in the Barents Sea area during the month of March, while the second phase took place in the Fram Strait where several aircraft surveys were conducted. The second part was also called CryoVex 2003, where the aircraft survey co-ordinated by the European Space Agency. Coincident, synchronous helicopter flights were carried out with a Danish Twin Otter fixed-wing aircraft equipped with a synthetic aperture radar altimeter resembling the new-generation SIRAL radar altimeter on board ESA's upcoming CryoSat mission in 2005. Sea ice thickness measurements were carried out using helicopter-borne electromagnetic induction and laser measurements. Furthermore, a number of other observations including ice coring and snow sampling, visual ice observations, video, photography and satellite image acquisition. A first prototype of an Automatic Ice Station measuring low frequency oscillation of the ice field was tested during the experiment

Table 1. Summary of non-space methods of ice thickness measurements used in cal-val experiments

Acronym	Characterization of the method	Partners
EM	Electromagnetic induction combined with laser altimeter, mounted on helicopter or from a beam mounted in the bow of an ice-going vessel. Well-established method which has been used for several years. A Geonics EM31 induction instrument is also operated from ice-going vessels and from sledges.	AWI
Airborne Laser and GPS	Airborne laser profiling and scanning combined with kinematic GPS from aircraft. Ice freeboard can be measured along the flight tracks in single-beam mode, giving a profile of ice thickness. In scanning mode a swath of ice heights is obtained, giving detailed information on ice ridging, lead geometry and ice rafting in a band along the aircraft trajectory, typically 300 m wide.	DNOSC
Ground penetrating radar	RAMAC GPR instrument operating at high frequency (above 50 Mhz) operated from a sledge, providing data similar to seismic measurements	AWI
IN SITU snow and ice data	In situ measurement of ice thickness, freeboard, snow cover, etc. from expeditions and ice camps	NERSC, AWI, NP

The different validation parameters and the measurements needed to obtain data are listed in Table 2. Also the contribution from the team members to provide is indicated in the table.

Table 2. Validation parameters

	<i>Volumetric Measurements</i>	<i>Drilling holes</i>	<i>Surveying</i>	<i>Scanning Laser</i>	<i>EM Sounding</i>	<i>Video Records</i>
Platform	In situ & ships	In situ & ships	In situ, sledge, ships	Aircraft	Helicopter, ships	Aircraft, helicopter, ships
Snow Density	X	X				
Snow Thickness		X				
Ice Density	X	X				
Freeboard		X	X	X	X	
Surface Topography			X	X	X	
Ice Thickness		X			X	
Floe Size				X	X	X
	AWI, NERSC, NP	AWI, NERSC NP	AWI	DNESC	AWI	DNESC

Satellite images from SAR, optical and infrared sensors were used for general mapping of the ice conditions (ice concentration, multiyear and firstyear ice, ice drift, ice floes and leads) in the study area (Figure 2). In particular Wideswath SAR images from ENVISAT were used both for planning of field measurements and for comparison of ice types with profiles of laser and radar data from aircraft. MERIS and AVHRR data were obtained every day when cloud conditions were good, while SAR data were obtained at least every 3rd day. Also low resolution data from passive microwave and scatterometer were obtained.

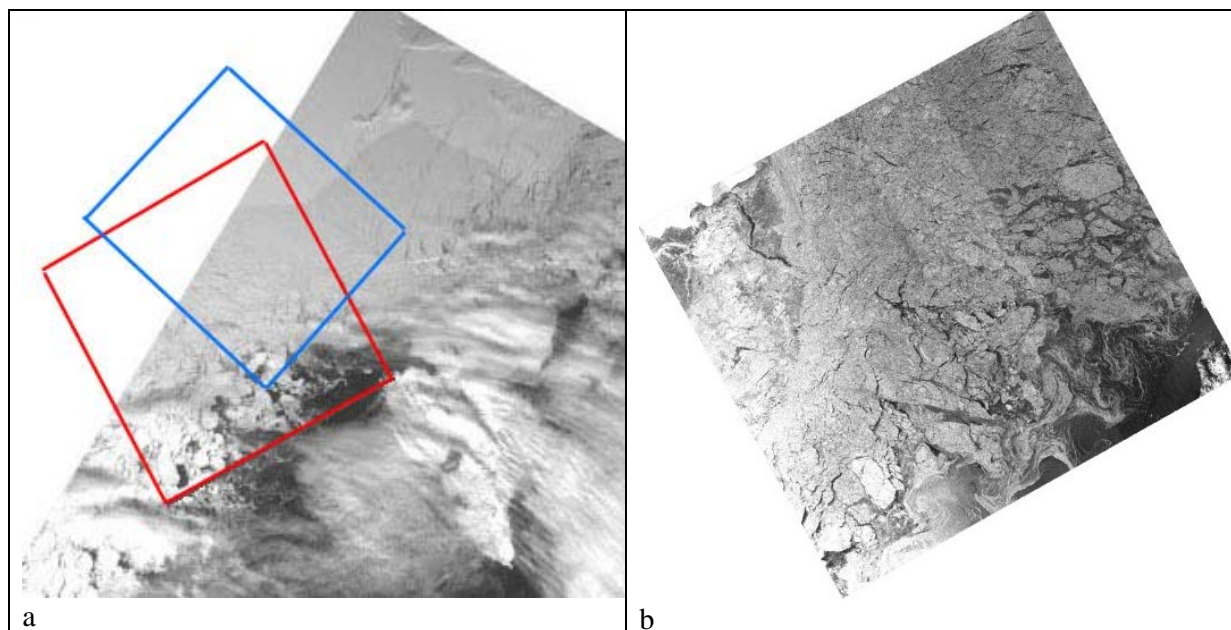


Figure 2. a) Subset of a MERIS image obtained in the CryoVex period (5 – 21 April) with the rectangles showing the location of ASAR Wideswath images on 11 April (red) and 15 April (blue) when dedicated aircraft surveys over sea ice were conducted; b) ASAR Wideswath image from 11 April.

1.2 Physical foundation: isostatic equilibrium of ice floating on water

The fundamental relations between the main ice, snow and ocean parameters are illustrated in Fig. 3, where isostatic equilibrium is assumed for ice floating on water. The density ratio, R , which is determined by the density of ice, snow and water, can be used to retrieve thickness from freeboard. The variability of R needs to be established. From literature, the following estimates are given:

$R = 9.1$ assuming no snow (Rothrock)

$R = 8.7$ Beaufort Sea in Spring (Bourke, Paquette, 1989)

$R = 7.8$ Direct measurements of draft and freeboard (Wadhams, 1991)

R is dependent on ice thickness

For $H = 2$ m, the freeboard is typically 20 - 30 cm, depending on snow cover and density. Results from ice thickness calculations and other CryoVex data analysis in the region north of Svalbard are presented in chapter 6.

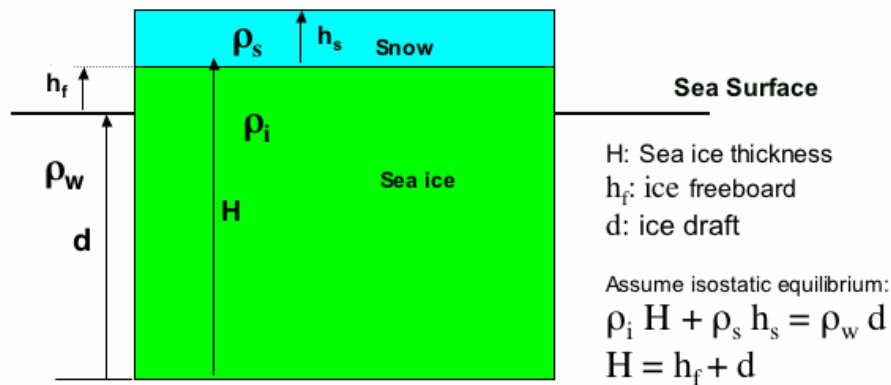


Figure 3. The relation between ice thickness, freeboard and density for snow-covered ice

1.3 Basic concepts of CryoSat sea ice thickness retrieval

The basic method of computing sea ice thickness by altimetry is to measure freeboard (that is the height of the ice or of the snow surface above water) from the difference between: a) the surface height of the larger ice floes, and b) the height of the thin ice or water surface in the major leads. Both heights may be referred to a common fixed surface (ellipsoid or geoid), but with sufficient small distance between major leads, this is not necessary to get the difference. In this context, an ice floe is a reasonably thick and old piece of ice, usually but not necessary MY (multiyear) ice. In the winter season, almost all leads are covered with thin ice, while in summer the leads are mostly open.

The SAR-altimeter is a new concept where the "footprints" of each single measurement is reduced to 200m along track from the pulse-limited altimeter footprint of some km, by use of the SAR (or doppler-history) principle. In cross-track direction, the footprint is the same size as determined by the currently operating pulse-limited radar altimeters (on ERS, Envisat). The shape and strength of

individual footprint pulses are analyzed and pulses are classified as representing footprints filled with:

- 1) thick ice,
- 2) leads (with thin smooth ice or calm water),
- 3a) mixed thickness ice and/or leads or 3b) medium-thick ice.

Separating the pulses into these three classes is made by analyzing the pulse amplitude and shape. High-peak return pulses with a steep and short trailing edge are classified as coming from leads (due to near-specular reflection from a smooth ice /water surface scattering), while low-peak pulses with a longer gentle-sloping trailing edge are classified as coming from thick ice floes (due to diffuse reflection / scattering from the generally rough ice surface and volume scattering). In addition to this major lead / ice pulse difference, which have been used previously to successfully analyze ERS altimeter signals (Laxon 1994, Wingham et al., 2001), also the pulse-power variation with incidence angle along-track will be available in the SIRAL Level 1b data, and is expected to be of additional help.

Class 3 pulses are discarded as coming from footprints with mixed thick ice / leads or from intermediate (medium thickness) ice types. Ice freeboard height to be used in subsequent calculation of MY ice thickness is determined from the pulses of classes 1 and 2, using the difference in timing of the leading-edge of these pulses.

1.4 Error estimates

The expected errors and possible corrections of the resulting ice thickness measurement are divided into two main groups:

- 1) Instrument related errors called **System-errors** in the conversion of measurement Level-0 data to pulse-data of level-1b.
- 2) Surface physics-and-modeling related errors called **Retrieval errors** in the conversion of Level-1b data into ice freeboard and then into ice thickness in Level -2 and level-3 data.

The total error of resulting ice thickness is the sum of errors in groups 1) and 2). The first group of errors will be addressed by the pre-launch **Calibration programs** followed by the post-launch **Verification program**. The second group is addressed by the pre- and post-launch **Validation programs**.

In this context, Cryovex03 is part of the pre-launch validation program for the CryoSat SIRAL instrument operated in the SAR-mode over Arctic sea ice.

The following expected retrieval errors and possible corrections can occur:

Reflection layer uncertainty

The altimeter operates at 13GHz. At this frequency, a dry snow layer of moderate thickness (generally less than 1m on the Arctic ice) is almost transparent to the radiation. Therefore, the main signal during winter is expected to come from the ice layers close to the snow-ice interface. This layer produces the main (volume-) backscattered microwave signal. Possible offset from the upper ice surface is unknown, but expected to be relatively small. Further studies are need to investigate the penetration of radar waves at 13 Ghz into the ice as function of temperature and salinity. This

is particular relevant for MY ice where volume scattering is significant. The measured height is called the ice-freeboard. This is in contrast to the reflection of the optical pulse from a laser altimeter. Here the signal is reflected close to the upper snow surface. The measured height is thus called the snow-freeboard.

Snow-load correction and error

A two-layer model of the sea ice, consisting of a snow-layer of uniform density (about 0.35) on top of the ice with density about 0.9 floating in water with density 1.025, is used. The ice thickness is computed from this model by input of the appropriate densities, the snow-thickness and the freeboard height.

Heavy snow on the top of the ice can lower the ice-freeboard considerably from that of a snow-free condition (it may even become negative in Antarctica!) It is therefore of great importance to have as good estimate as possible of the snow-load. This value is not in itself measured by the CryoSat satellite and has to be estimated.

The Preferential Sampling effect

As explained above, the footprints used for calculating the ice freeboard will mainly be over the large ice floes, since the signals from mixed ice -lead footprints are discarded. This means that only floes at least 1- 2km across (details depending on the footprint/ cross-track geometry) are measured. Intermediate ice (with thickness between thin ice in leads and MY ice) will tend to be discarded from the freeboard analysis and the subsequent ice thickness calculation. Discarding smaller floes and mixed /thinner types of ice may introduce a bias relative to the simple area-average ice thickness. This is due to the fact that the intermediate thick ice can be assumed to be found in older leads of smaller size. Thin ice is less of a problem and of course also used as the instrument surface reference. However, the exclusion of smaller floes is not necessary a retrieval error, since the SIRAL-measured ice freeboard is used mainly to calculate the thickness of the thicker (or MY) ice.

In this connection, note that the simultaneous measurement of the ratio of FY to MY ice, e.g. by using the passive microwave radiometers SSMI and AMSR, can be very helpful in correcting for this bias. It is also of interest in the pre-launch validation to relate the ice thickness with the floe size (as a joint probability function of floe area and ice thickness. Co-located measurements of freeboard (by Laser or thickness by EM) with imagery of the floe size by visual aircraft imagery can be used for this.

Other expected error sources

- The ice density will vary, introducing noise and possible bias. This is discussed in chapter 6.
- Timing of the pulse leading-edge may depend systematically on the pulse-shape (lead-pulse or ice-pulse). Corrections here should be included in the processing algorithm.
- Most large ice floes are not level, and undulations (ridges) will introduce noise. No serious bias is expected from this as ridges will be included in the ice thickness defined.

2. Aircraft data

The Danish National Space Center (DNSC, former KMS) operated an airborne laser scanning system which was mounted in the Air Greenland Twin-Otter aircraft in Nuuk, Greenland before the CryoVex campaign in April (Fig. 4). Kinematic GPS is the key positioning method for the aircraft. GPS dual-frequency phase data were logged at 1 Hz using 1-2 reference ground receivers at one or more reference sites, and 3 aircraft receivers (Trimble, Ashtech and Javad types). In addition GPS data were logged at a number of reference sites in the airports. In addition, an interferometric radar altimeter (D2P) from John Hopkins University, Applied Physics Laboratory, USA was installed to obtain data similar to the CryoSat SIRAL. After all the installations were successful done, and the CryoVex flight campaign was initiated on April 7. A total of 61 hours were flown at a nominal flight elevation of 1000 ft, including additional flights off Station Nord, on the Geikie Ice Plateau off Mestersvig and in Nordaustlandet on Svalbard (Table 3). Dedicated sea ice flights around “Polarstern”, were conducted on 11, 15 and 17 April. The flight tracks for the whole campaign are shown in Fig. 5.



Figure 4. Air Greenland Twin-Otter at Mestersvig

A Honeywell medium-grade embedded GPS and inertial navigation system H764-G “EGI” was used throughout the flights to record inertially integrated position, velocity and attitude information. Both free-inertial and GPS-integrated inertial data were logged on many flights. Data volume per flight was typically 50 MB/hour. Nearly all EGI data were recovered. The DNSC Riegl laser scanner (lidar) data was logged as hourly files on a stand-alone laptop computer. The lidar files were time tagged by a 1 pps signal from the AIR1 GPS receiver, with start time of the scans given by the operator as a file name. Nominally files covered about 1 hr of data, at 40 scans/second and 200 measurements per scan. No data was taken in fog. The lidar data were processed by merging with GPS positions and EGI attitude data, an example of the lidar ice surface height data is shown in Fig. 6. In addition to laser and radar data, digital video and imagery data was also collected (Fig. 7). An example of co-located EM-data and the lidar data from the 11 April joint flight is shown in Fig. 8.

Table 3. Overview of the sea-ice and land-ice validation experiment flights. The dedicated sea ice flights are indicated in the shaded rows.

Date/Julian Day	Departure - destination	Track	Off bloc	Take off UTC	Landing UTC	On bloc	Airborne
April 5 / 95	SFJ-SFJ	test	1955	2011	2056	2100	0 h 45
April 7 / 97	SFJ-MRG	SJ1-EGIG	1255	1306	1812	1818	5 h 06
April 9 / 99	MRG-NRD	B	0936	0949	1438	1444	4 h 49
April 10 / 100a	NRD-NRD	D		1013	1529	1533	5 h 16
April 10 / 100b	NRD-NRD	E		1618	2137		5 h 19
April 11 / 101	NRD-LYR	N-PST-P1		0910	1444		5 h 34
April 15 / 105a	LYR-LYR	PST-P2		0950	1451	1455	5 h 01
April 15 / 105b	LYR-LYR	Austfonna		1552	1910		3 h 18
April 17 / 107	LYR-NRD	Bouy-grid	1215	1227	1754	1758	5 h 27
April 18 / 108	NRD-NRD	F	1016	1021	1618	1622	5 h 57
April 19 / 109	NRD-MRG	H	1027	1031	1458	1501	4 h 27
April 20 / 110	MRG-MRG	Geikie	1031	1033	1431	1435	3 h 58
April 21 / 111	MRG-SFJ	EGIG		1050	1710		6 h 20
TOTAL							61 h 17

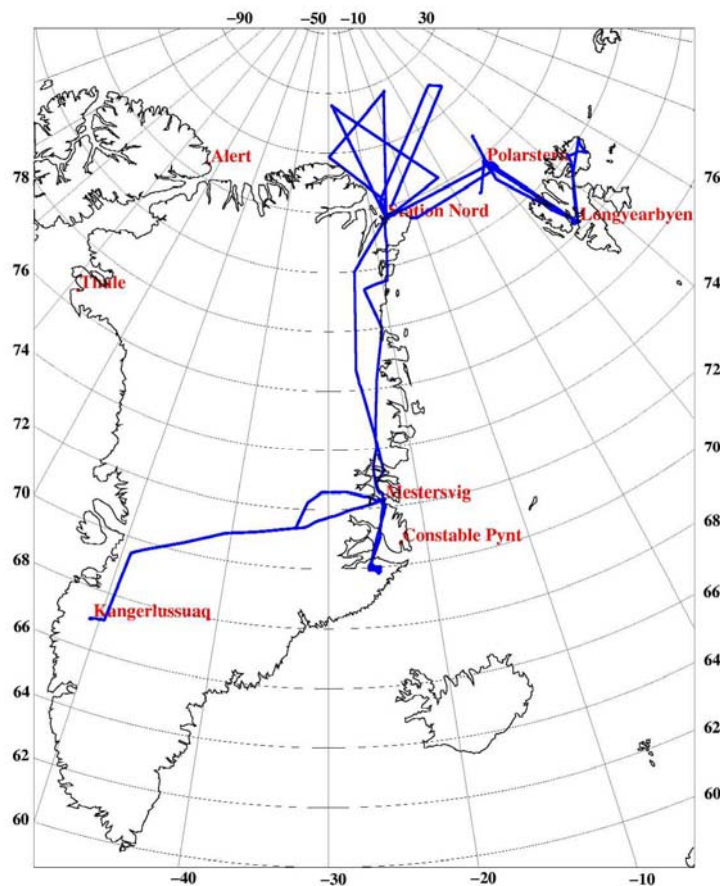


Figure 5. Flight tracks for the Twin Otter during the "CryoVex" campaign, April 2003.

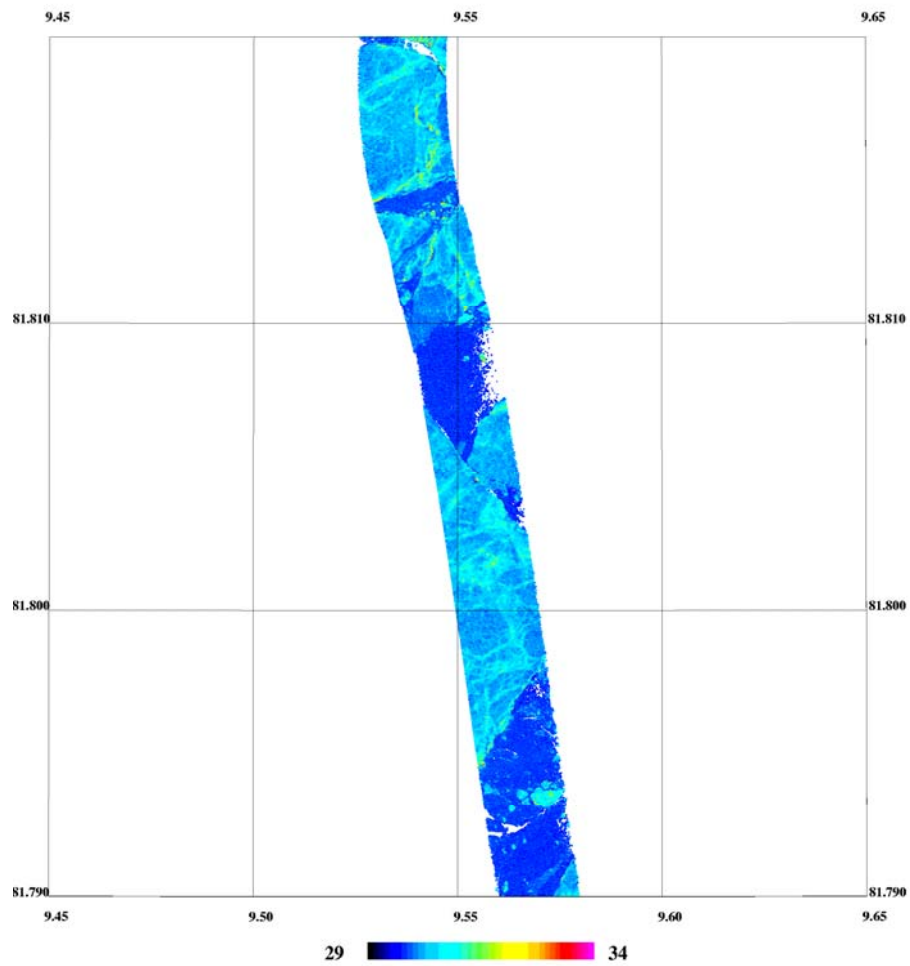


Figure 6. Example of lidar ice height data (ellipsoidal heights, meter) from 11 April. The swath width is about 300 m. Ice floes and their freeboard height are well distinguished from open water and thin ice.

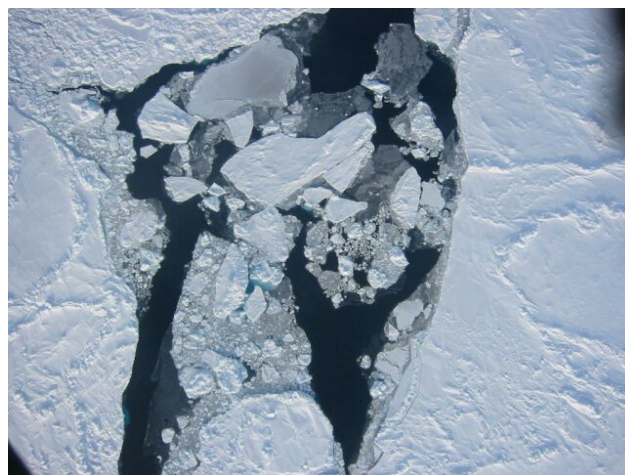


Figure 7. Example of vertical photos taken at 5 sec interval, yielding a near-continuous strip with swath width of about 300 m. The photos are used to verify ice floes, leads and ridges observed by the lidar

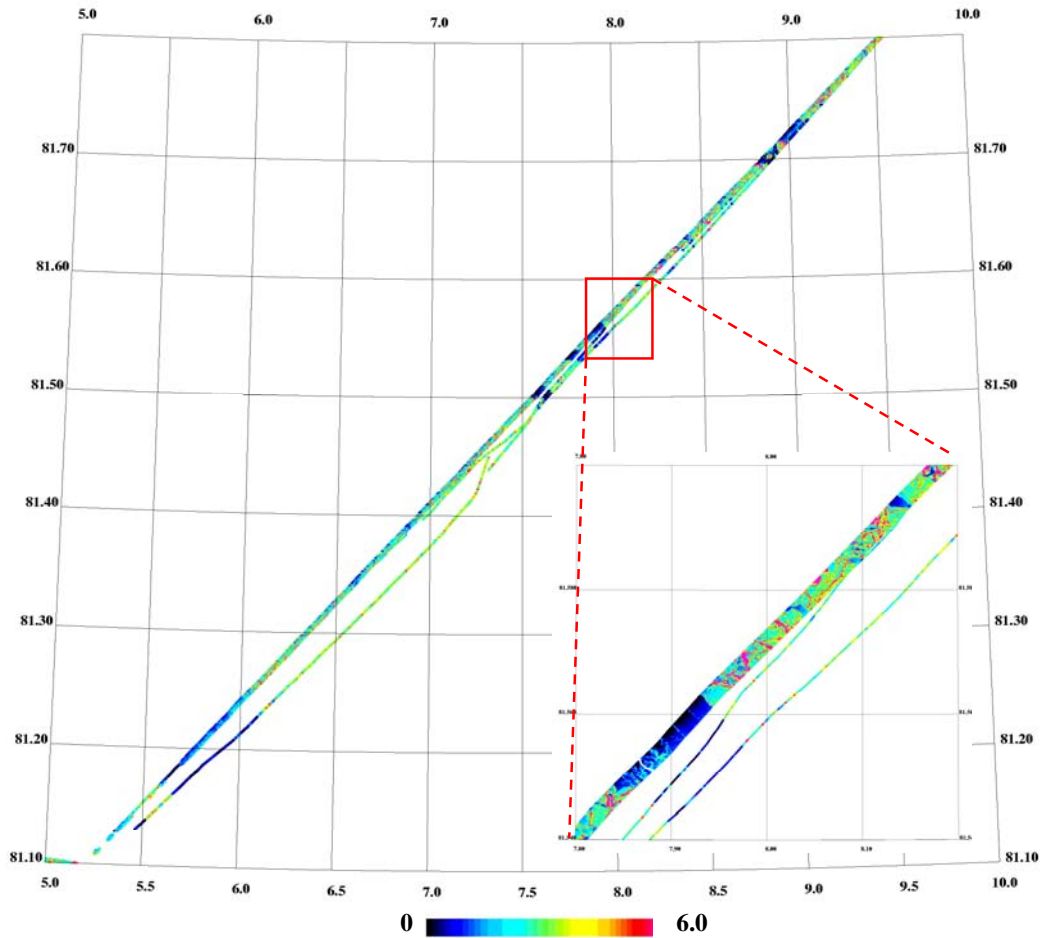


Figure 8. Example of simultaneous ice thickness by laser (broad swath) and EM helicopter (thin line) obtained on 11 April 11. Colours show ice thickness in meter. This represents the first cross-validation of the EM and laser methods. The co-location of the two flight lines was not as good as planned on this date, but it was improved on the next joint flight on 15 April.

3. Ice thickness measurements using helicopter and in situ techniques

The main goal of ice thickness measurements on the Polarstern expedition was to gain high resolution data to describe local and regional thickness distributions and surface morphology. Several observing methods are described which are based on electromagnetic (EM) induction sounding. The technique allows for continuous high accuracy measurements, performed either directly from the ice surface or from above, e.g. by means of the ship or helicopters.

With EM sounding, a low-frequency EM field is generated by a transmitter coil. This field induces eddy currents in the water, which in turn result in a secondary EM field. The strength of this field is measured by a receiver coil. As the strength of any EM field decreases with distance to the source, the secondary field strength decreases with increasing distance between the EM instrument and the water underneath the ice. Thus, the thicker the ice is, the weaker the secondary field becomes. Here, we deployed a hierarchy of different means of EM soundings: Ground-based measurements have

proven to provide very accurate data. Their calibration is evaluated by means of accompanying drill-hole measurements. However, ground-based measurements are only possible on single, thick floes, and the profile lengths are very limited. Another possibility is to perform continuous ship borne measurements along the ships track. These provide the most extensive data en-route without any extra requirement for ship time. However, the ice thickness along a ships track is never representative for a particular ice regime, as the ship usually follows leads with open water or new ice. At floe contacts, where the icebreaker has to break thicker ice, the ice is often deformed. Therefore we also carried out extensive helicopter borne surveys using a towed sensor, the EM bird.

3.1 Ground-based profiling using an EM31 thickness sensor

Ground-based measurements have been performed on a daily basis on single ice floes using a Geonics EM31 instrument. Floes have been entered either from the ship or by helicopter during floe-hopping, when several floes were profiled during one flight. The EM31 operates at a frequency of 9.8 kHz with a coil spacing of 3.66 m. The EM31 provides high accuracy data and the procedures are well established. The EM31 was placed into a Prijon kayak serving as amphibic sledge, to enable measurements over melt ponds and to shelter the instrument. EM soundings were performed at a lateral spacing of 5 m. The profiles were laid along straight lines, including level and deformed ice. The EM profiles were occasionally validated by means of drill-hole measurements when time and weather allowed.

Along the EM profiles, also snow thickness was profiled using a ruler stick. This provided essential data e.g. for CryoSat validation, as the obtained data allow to distinguish between snow and ice thickness.

3.2 SIMS (Sea Ice Monitoring System): Continuous along-track ice thickness measurements

Since 1994, continuous EM ice thickness measurements are performed along ship tracks. Since 2001 (Ark 17/2), a Geonics EM31 is used together with a Riegl laser profiler, and the system is integrated into Polarstern's PODAS system, called SIMS. During Ark 19/1, first tests were made integrating a KT15 infrared thermometer into the SIMS. The data were acquired with the turbulence measurements at the bow, and kindly provided by W. Cohrs (AWI).

Unfortunately, archiving of SIMS data into PODAS could still not be achieved, although the data were readily visible on the ships information monitors, including those on the bridge. Therefore, the navigation (GPS) data had to be joined with the thickness soundings only during post processing. However, synchronised and geo-referenced thickness, speed, and surface temperature data are available shortly after the cruise.

SIMS was operated continuously from 09 March until 19 April when Polarstern was steaming in ice. Calibration is an important duty in EM thickness profiling, and is required to assess the systems stability. In the beginning, an old calibration from 2002 was used, because no actual calibration could be performed due to the lack of extensive water patches or leads.

The first calibration was therefore only carried out on 23 March. During a five minute calibration experiment, SIMS was raised and lowered in a large lead above open water, and the according laser height and EM reading (apparent conductivity) was recorded (Fig. 9). The relationship between apparent conductivity and SIMS height above the water surface shows the well-known negative-exponential relation (Fig. 10). The curve has a very good signal-to-noise ratio except for some scatter between 4.5 and 6.0 m, which is due to some brash ice under the system. A calibration curve can be obtained by fitting a negative-exponential function to the data (Fig. 10). Inversion of this function yields a transformation equation to compute distance to the water surface from apparent

conductivity. Ice thickness is then obtained by subtracting the laser-measured height above the ice surface.

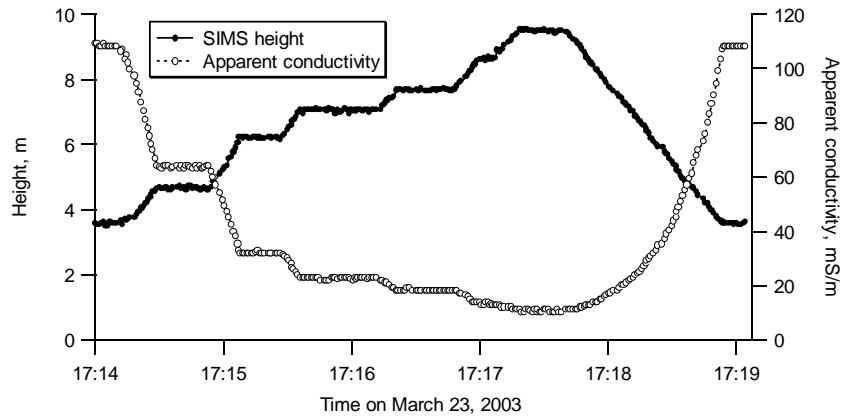


Figure 9: SIMS height and corresponding measured apparent conductivity during a calibration measurement, when SIMS was raised and lowered over open water.

The 2003 calibration agreed with the curve of Ark 11 in 1995, which was well explained by a one-dimensional model of a non-conductive ice cover overlying deep sea water with a conductivity of 2600 mS/m. The remaining discrepancy may be due to a different calibration factor of the particular EM31 used (e.g. a factor of 1.12 to account for instrument use at hip-height), but should be controlled by repeated calibration measurements. Deviations from the 2001 curve are quite significant, and point to an outbalanced (tilted) SIMS during 2001. The scatter of the curves demonstrates how important repeated and careful calibration measurements are. They should be performed also with future SIMS realisations.

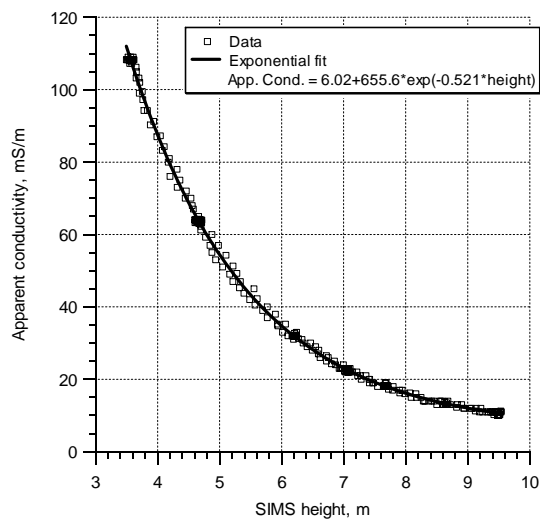


Figure 10: Apparent conductivity (EM31 reading) versus SIMS height during the calibration measurement of Fig. 9.

A typical thickness profile from SIMS is shown in Figure 11. The data were recorded during extensive ramming, showing the typical cycle of absent or thin ice and thick ice which brought the ship to a stop. Accordingly, the resulting thickness histogram shows two clear modes at 0 m and 1.6 m ice thickness (Fig. 12). The example illustrates the importance of co-registered GPS data, if the real thickness distribution of the regions shall be derived. This can only be obtained by removing all sections of the track when the ship was moving backwards or repeating a measurement over a formerly profiled spot. In fact, the typical thickness in the regions of the example was 1.6 m, explaining well the difficulties in moving straight forward.

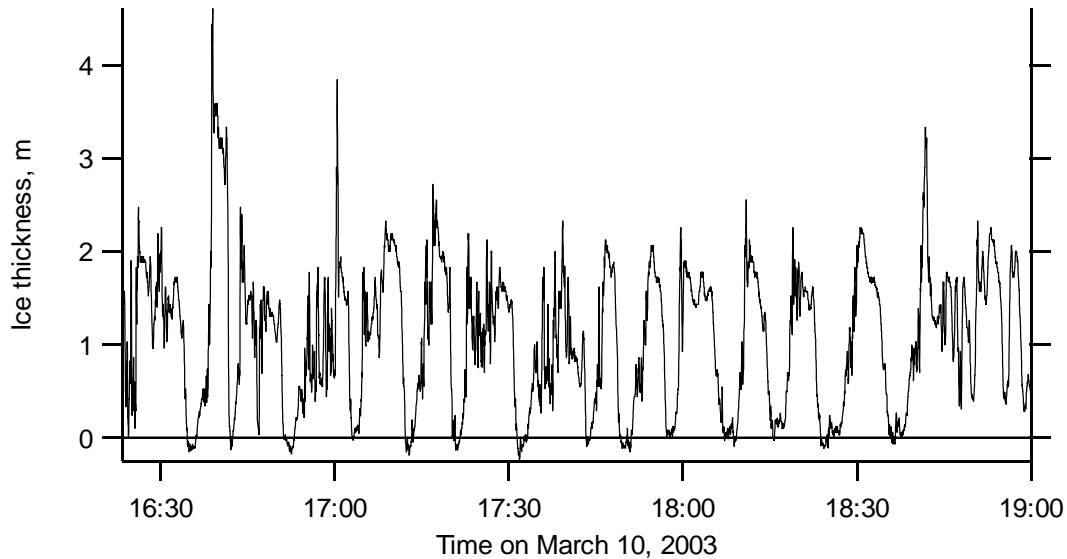


Figure 11: 2.5 hour recording of ramming cycles.

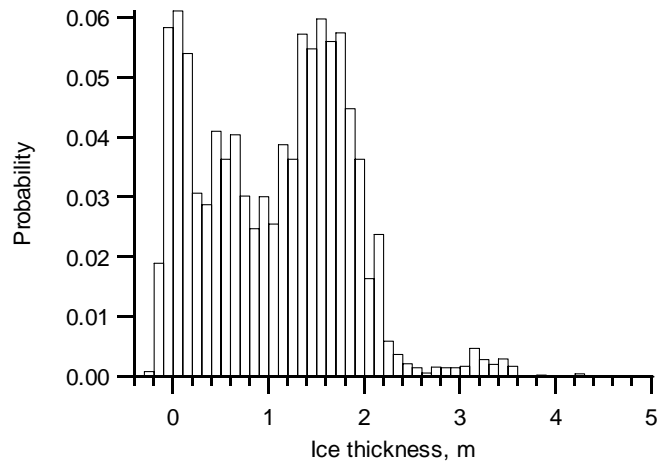


Figure 12: Thickness distribution for the example in Figure 11.

3.3 Airborne thickness profiling using an EM bird

A helicopterborne EM ice thickness sensor (EM bird) was operated with the Polarstern BO-105 helicopters during 21 flights. The bird is 3.5 m long, has a diameter of 0.35 m, and weighs about 100 kg. It is towed 20 m below the helicopter, at a height of about 10 to 15 m above the ice surface (Fig. 13 a). Take-off and landing were conducted from the helicopter deck. The bird was successfully landed directly into a special cart which could also be used for transport and storage on board.

The bird operates at 3.68 and 112 kHz, with coil spacing of 2.77 and 2.05 m, respectively. A GPS antenna and a laser altimeter are also included. Flights were performed along triangles with 40 km side length. At each turning point, the helicopter ascended to an altitude of 100 m to allow for internal calibration and resetting of the bird. Some flights were complemented by ground validation along coincident short profiles on the longer ice stations close to the ship.

A nadir video camera was operated during all video flights to document ice conditions below the bird. However, on most flights videos were only recorded during the high altitude sections to limit the amount of video data and to document general ice conditions in the region. Geo-referenced digital still photographs were also taken to document general ice conditions. Subsequently they were included into an html linked map projection allowing for easy geocoded image browsing. All the flights are summarised in Table 4, and the tracks north of Svalbard are shown in Fig. 13 b.

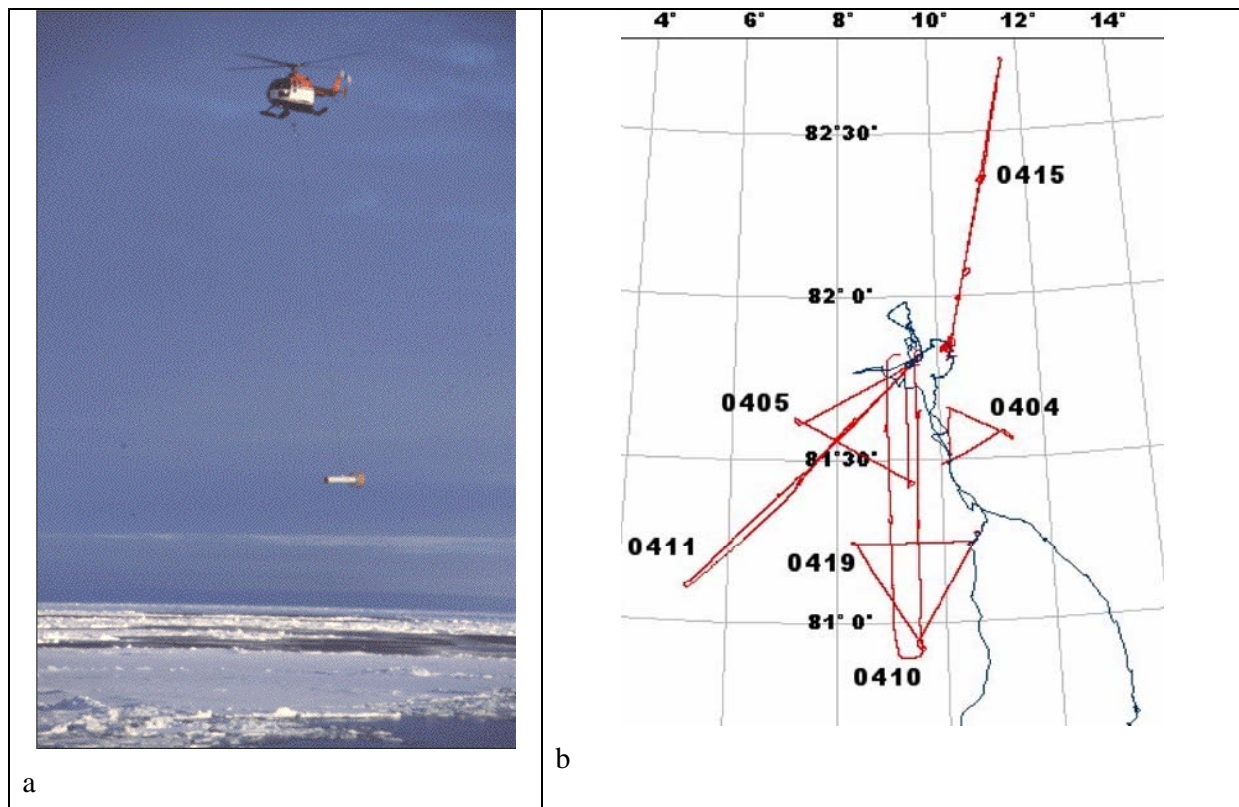


Figure 13. a) Photograph of the HEM system in operation; b) map showing the HEM flight tracks (red) and the Polarstern tracks (blue) during the CryoVex campaign north of Svalbard.

Table 4 : Dates and starting positions of helicopter EM thickness surveys

Date	Latitude	Longitude	Comment	Date	Latitude	Longitude	Comments
06.03.2003	75.81	17.26	MIZ	01.04.2003	80.43	12.83	Ground contact
10.03.2003	76.79	19.09		04.04.2003	81.49	10.18	
12.03.2003	76.81	20.17		05.04.2003	81.79	9.47	
15.03.2003	77.21	20.45		10.04.2003	81.81	9.68	
16.03.2003	77.56	20.33		11.04.2003	81.81	9.60	First CryoVex flight
17.03.2003	77.54	20.38	Inner Storfjord	14.04.2003	81.84	10.28	Grid over station floe
21.03.2003	76.63	19.61		15.04.2003	81.84	10.29	Second CryoVex fl.
22.03.2003	76.44	21.87		19.04.2003	81.27	10.57	
23.03.2003	76.26	23.19		21.04.2003	79.40	3.35	Calibration over open water
24.03.2003	75.96	25.51					
25.03.2003	75.88	27.51					

Several profiles of data from EM-bird obtained in 2003 have been processed and analysed. Figure 14 a shows an example of a profile of about 8 km in length, where the upper graph is the surface height measured by the laser and the lower graph is the ice draft measured by electromagnetic induction. Figure 14 b shows a shorter profile of ice draft, about 1.4 km, where validation has been performed over a distance of 200 m by ground penetrating radar mounted on a sledge. Additional validation was performed by drilling wholes along the profiles.

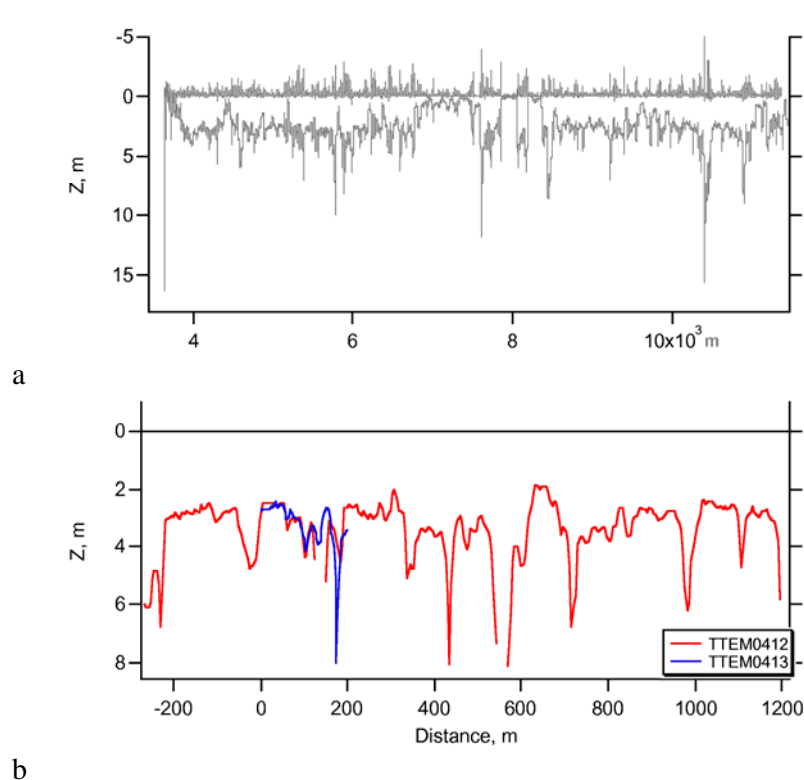


Figure 14. Example of EM-bird data from the section obtained on 11 April 2003, a) shows surface elevation from the laser (upper graph) and ice draft from the EM induction method, b) shows a comparison of EM draft data (red curve) with ground penetrating draft data (blue curve).

3.4 Ground penetrating radar

During ARK 19/1 a RAMAC Ground Penetrating Radar (GPR) instrument (MALA GeoScience) was taken to the sea ice for the first time to assess the capability of the method to contribute information on the sea ice properties particularly ice thickness (Fig. 15).



Figure 15. RAMAC GPR mounted into a little Pulka.

In contrast to EM induction methods, GPR systems use a high frequency (> 50 MHz) electromagnetic pulse comparable to seismic acoustic shots. If there are changes of the dielectric properties of the media on distinct horizontal layers, the EM pulse is partly reflected and returns to the receiver antenna of the system. An example for such a horizontal layer would be the ice underside where the media changes from ice to water.

Once the antenna has transmitted the EM impulse the receiver starts to acquire the returning signals for some nanoseconds. For interpretation the signal traces of every shot are plotted next to each other in a radargram (Fig. 16). The grayscale displays the amplitude of the received waveform. After the reflected waveform of the ice underside is identified, the travel time of the wave down and up can be derived (between 20 – 30 ns in this example). With the help of drilling information or using standard values for the propagation velocity, the travel time can be converted into ice thickness. In Figure 16 the bars represent the drilling information.

The propagation velocity depends on the dielectric permittivity of the media. The reflectivity is related to changes in the dielectric properties, determining the velocity. Apart from the wave travel velocity, the damping of the wave depends on the conductivity of the media and the antenna frequency (50 MHz up to 1.5 GHz). Damping increases with frequency and conductivity.

In Figure 16 a dominant reflector corresponds nicely with the drilling information. A second reflector at around 10 ms maps the snow-ice interface as the antennas are pulled over the snow surface. Only where the ice gets too thick or consists of many little broken pieces it is difficult to find a reflected signal in the data. For comparison the EMI derived ice thickness for the same profile as in Figure 16 is shown in Figure 17. The circles represent the drilled thickness like the bars in the radargram.

Due to its wave characteristics and the small point spacing GPR provides results with higher lateral resolution and accuracy. However, dealing with high salinity ice or not level ice conditions as e.g. pressure ridges, there are problems to retrieve ice thickness information which can be solved with the EM method.

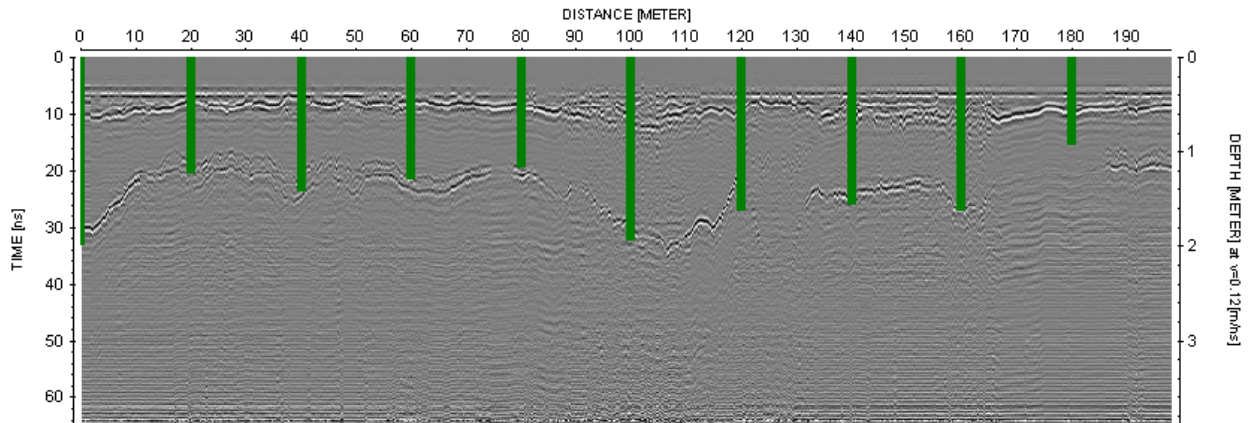


Figure 16: GPR section (radargram), Antenna: shielded 800 MHz, Date: 20030312. Drilling information plotted as black bars.

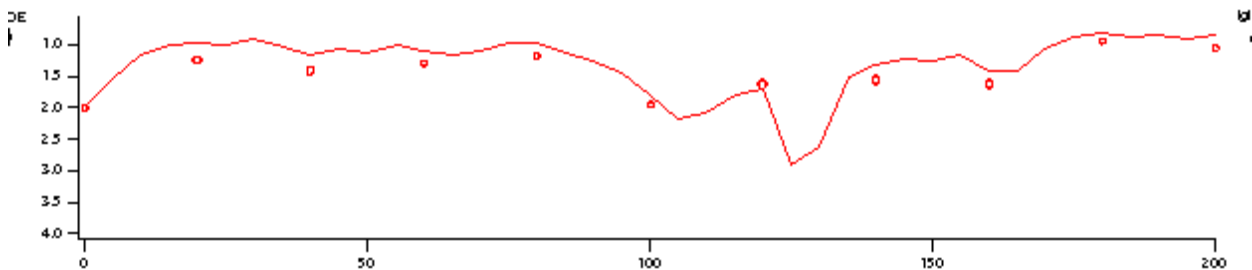


Figure 17: EM-derived ice thickness (lines), circles represent drilling data. Date: 20030312. Spacing: 5m.

3.5 Results from the Barents Sea and Storfjorden

Helicopter surveys and in situ measurements were conducted in the Barents Sea and Storfjorden as shown in Fig. 18. From SAR imagery and ice core analyses, the ice in the study area was a mixture of second-year and multiyear floes from the Arctic Ocean, and deformed first-year ice formed locally. Only few cracks and narrow leads led to the inner Storfjorden, where grey ice with thin or no snow prevailed. By means of ground measurements and EM flights, much of the Storfjorden and an almost continuous section across the Barents Sea could be profiled. In total, we sampled 24 floes and performed 12 EM flights.

The results are summarised in Fig. 19 where ice and snow thickness obtained from ground-measurements is plotted versus latitude, i.e. a pseudo profile along Storfjorden and the neighbouring Barents Sea. In Storfjorden, no clear thickness trends from N to S are visible. However, it should be noted that due to the cruise track no measurements were possible in the first-

year ice produced in Storfjorden. Typical thicknesses between 0.6 and 1.0 m are in partial agreement with the airborne thickness distributions presented below. However, it becomes clear that the ground measurements were much too sparse to be representative for the overall thickness distribution. In the Barents Sea, a gradual thinning towards the ice edge is visible. However, older and younger ice cannot be separated based on the thickness data alone.

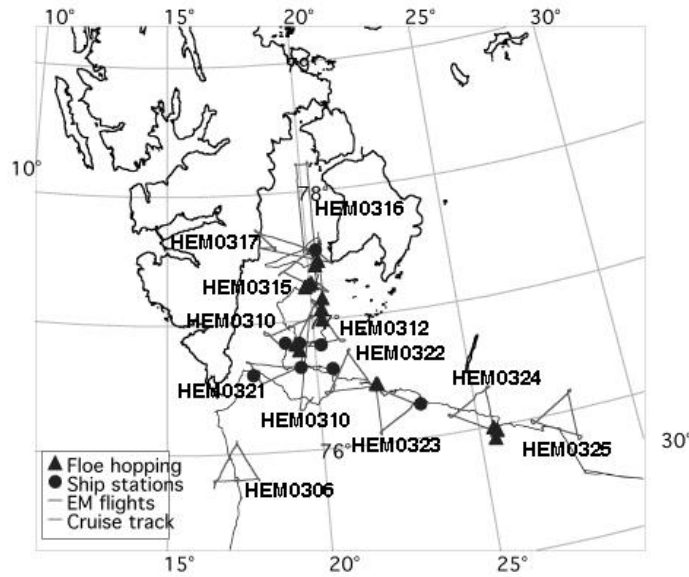


Figure 18: Map of Storfjorden and Barents Sea, showing the locations of ground measurements and tracks and dates of helicopter EM flights.

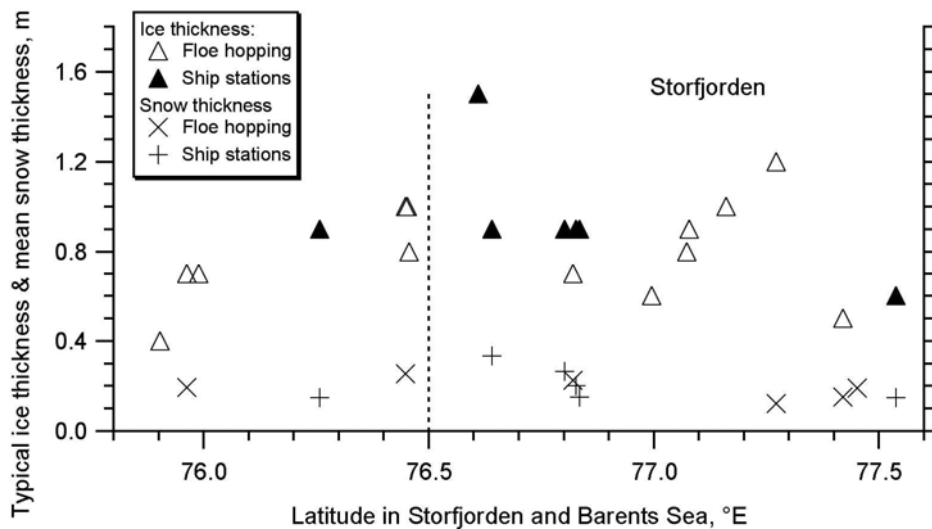


Figure 19: Typical ice and snow thickness obtained from ground-measurements versus Latitude, between Barents Sea (left) and Storfjorden (right).

Data from the EM flights were used to distinguish between the areas of thin ice formed in Storfjorden and the thick ice advected from the Arctic Ocean. Figure 20 shows a comparison of different ice thickness distributions obtained on Flights 0316 (a), 0315 (b&c), and 0312 (d), showing the transition between the different ice regimes. While the grey ice in inner Storfjorden was only 0.2 m thick, the thick ice further to the south had typical thicknesses up to 2.3 m. The modes at small thicknesses represent nilas formed on open water leads. Figure 21 shows the transition between the different ice regimes, which was encountered on the W-E flight on 0312. The corresponding thickness distribution is shown in Figure 20 b.

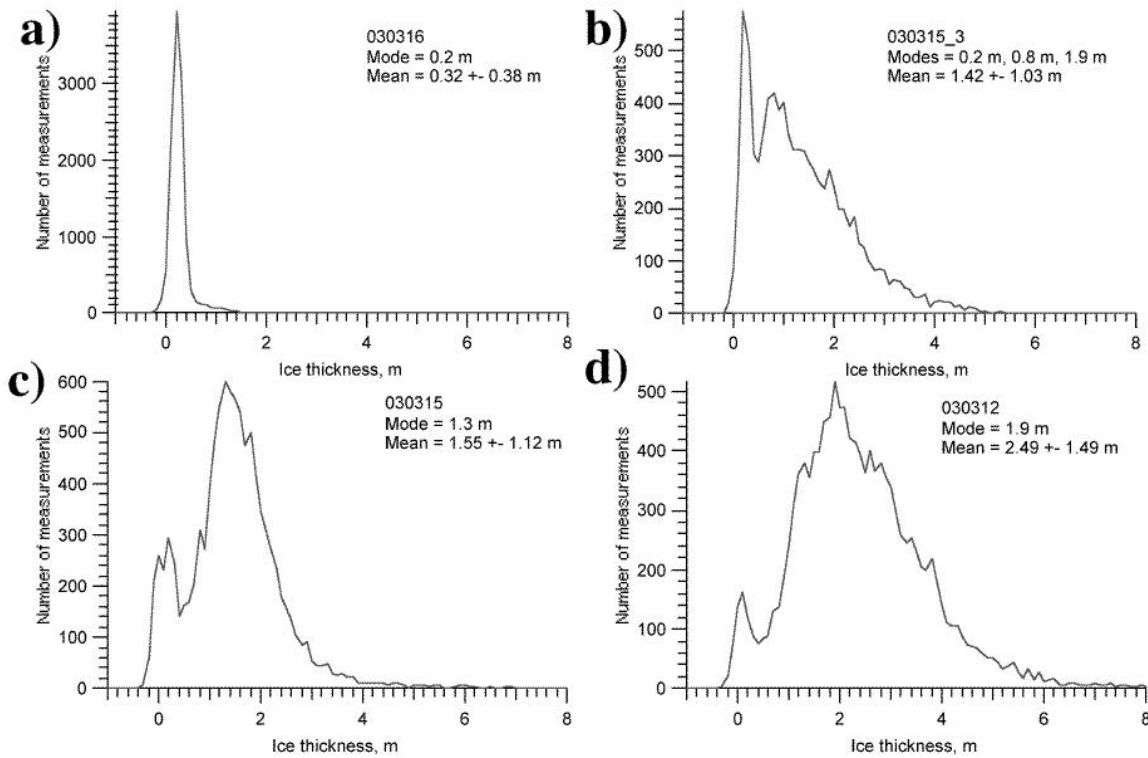


Figure 20: Ice thickness histograms for different flights in the Storfjorden area (see text) mapping different ice regimes.

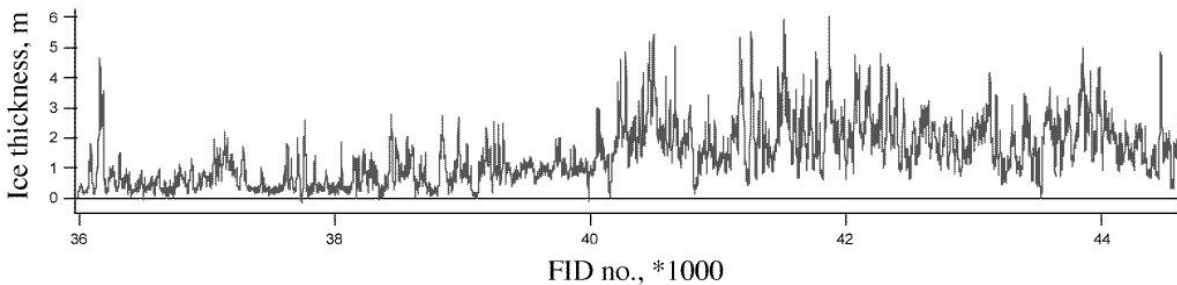


Figure 21: Thickness profile obtained on March 12 showing the transition from thin first-year ice into thick second- or multiyear ice.

3.6 Laser profiling of pressure ridges

Pressure ridges are the most significant features of sea ice roughness. Ice floes, which collide due to wind forcing or swell, tend to pile up in so called ridges. Ridges are separated into an upper part, the sail, and a lower part below the ice or water surface, the keel. Both features are important for momentum flux from atmosphere and ocean to the ice. Typically the keel is about 4 times deeper as the sail high and also 2-3 times wider.

The laser measurements performed with the EM bird can be processed to obtain height, width and spacing of pressure ridges. During the first part of the cruise in the Storfjord region 12 and during the second part north of Svalbard and north of Fram Strait 8 helicopter flights were performed. The flight tracks ranged from 60 km to 200 km and were in most cases shaped like triangles with equally sized sides. With an intermediate flight speed of 60 knots and a sampling frequency of 100 Hz point spacing results in 0.3 m. The instrument was usually flown about 15 - 20 m above the ground.

The processing of the laser data is complicated by variably vertical motion of the helicopter. That is why the raw data has to be high pass filtered first in order to fit a curve of the helicopter movement. In a second step a profile of the surface is derived. Furthermore mean height, width and spacing of pressure ridges and their number per km along the flight track is calculated as well as width and number per km of ice floes and leads. To define individually identifiable ridges a Rayleigh criterion is used which means that a single ridge must have a crest elevation of more than double the height of the surrounding troughs.

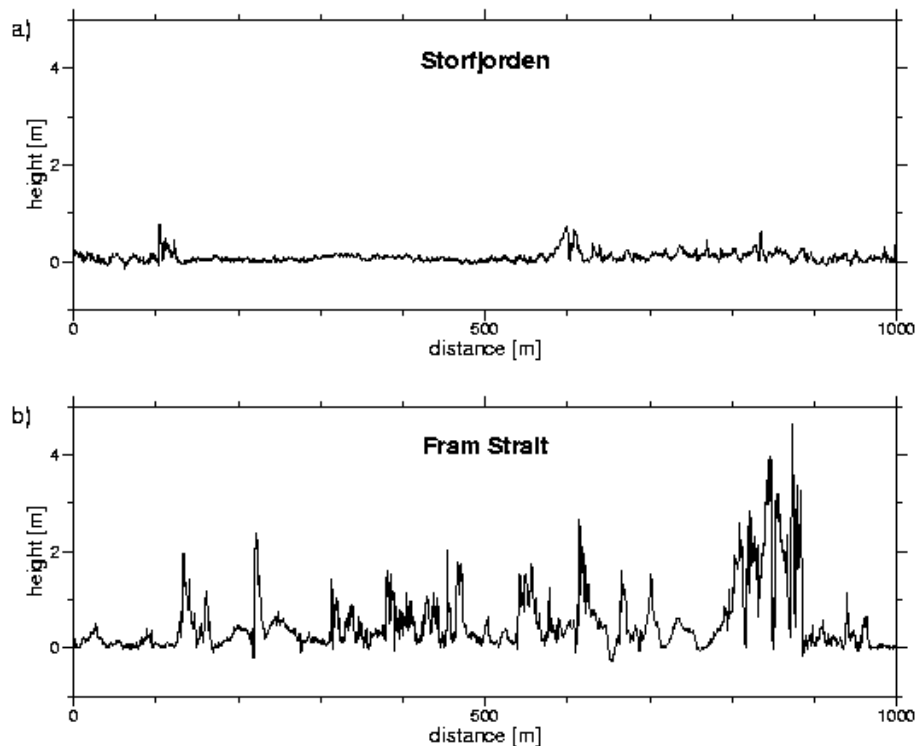


Figure 22: Comparison of laser derived surface roughness of undeformed grey ice in Storfjorden (a) and heavily deformed multiyear ice in Fram Strait (b). The Fram Strait profile is from the first CryoVex flight.

Besides being an Arctic winter expedition this cruise features measurements of young and first year ice on the one hand and multiyear ice on the other hand. The typical difference in surface roughness as revealed by the processed laser data is shown in Figure 22, comparing level grey ice in Storffjorden with heavily deformed multiyear ice in Fram Strait. Preliminary results show that ice floes in Fram Strait were 30 times larger in diameter than the floes in Storffjorden (100 m average). However, ridge frequency was similar in both regions, amounting to about 22 ridges per km. The smaller floes in Storffjorden allow wind and oceanic currents to produce more leads. The data show a two orders of magnitude higher number of leads in the Storffjorden compared to the Fram Strait profile.

4. In situ measurements of sea ice and snow parameters

Hourly, standardised visual ice observations were performed in a joint effort by all 16 sea ice scientists during daylight hours when the ship was moving through ice. In total, 279 observations were performed. On board, all observations and photographs were typed into Excel spreadsheets and linked to the home pages of AWI

4.1 Ice coring by AWI

Supported by the biological sea ice group 10 ice cores were obtained on different floes visited during thickness work. They were analysed for crystal texture and salinity to better judge age and origin of the sampled floes. In fact, only through these analyses a clear picture of the different young and old ice regimes arose which was not so clear based on thickness profiles alone.

Figure 23 illustrates the typical C-shaped profiles of first year ice from the Barents Sea and the almost fresh ice typical for multiyear ice in Storffjorden. On 16 March the ice floe consisted of an old floe rafted over a first-year floe.

The in situ observing positions are summarised in Table 5.

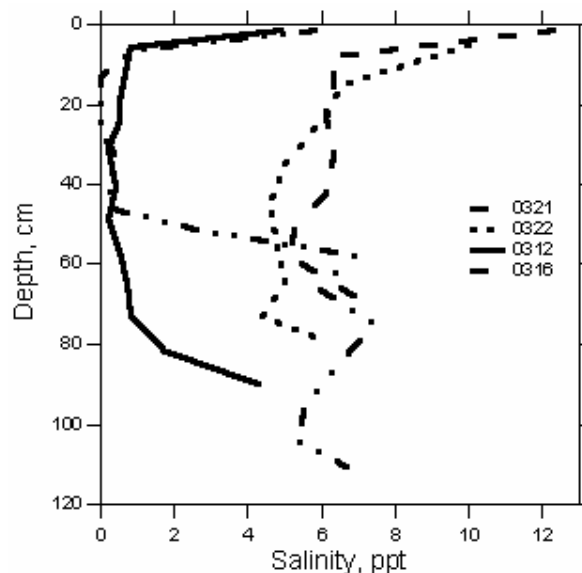


Figure 23: Typical salinity profiles of four ice cores obtained in Storffjorden and the Barents Sea.

Table 5a: Dates and locations of extended ground-based thickness profiles

Date	Latitude	Longitude
08.03.2003	76.61	20.55
09.03.2003	76.64	19.50
10.03.2003	76.84	19.03
11.03.2003	76.83	19.51
12.03.2003	76.80	20.23
17.03.2003	77.54	20.34
23.03.2003	76.26	23.28
01.04.2003	80.42	12.82
07.04.2003	81.90	9.57

Table 5 b. Dates and locations of short ground-based thickness profiles from helicopter floe hopping

Date	Floe No.	Latitude	Longitude
14.03.2003	1	77.00	20.35
14.03.2003	2	77.08	20.36
14.03.2003	3	77.16	20.42
14.03.2003	4	77.07	20.38
15.03.2003	1	77.42	20.28
15.03.2003	2	77.45	20.40
19.03.2003	1	77.28	20.09
19.03.2003	2	77.27	19.98
19.03.2003	3	77.26	19.86
21.03.2003	1	76.82	19.39
21.03.2003	2	76.77	19.49
22.03.2003	1	76.45	74.11
22.03.2003	2	76.46	21.92
22.03.2003	3	76.45	21.97
24.03.2003	1	75.96	25.58
24.03.2003	2	75.99	25.48
24.03.2003	3	75.90	25.49

Table 5 c: Dates and locations of ice core samples

Date	Latitude	Longitude	Comment
08.03.2003	76.61	20.55	
12.03.2003	76.80	20.23	
15.03.2003	77.42	20.28	
16.03.2003	77.54	20.34	
19.03.2003	77.28	20.09	
21.03.2003	76.82	19.39	
22.03.2003	76.45	74.11	
23.03.2003	76.26	23.28	
09.04.2003	81.85	9.68	Only 1.5 m surface core
12.04.2003	81.85	9.93	Only 1.5 m surface core
15.04.2003	81.81	10.25	new ice
16.04.2003	81.78	10.27	same new ice as above
17.04.2003	81.75	9.96	same new ice as above

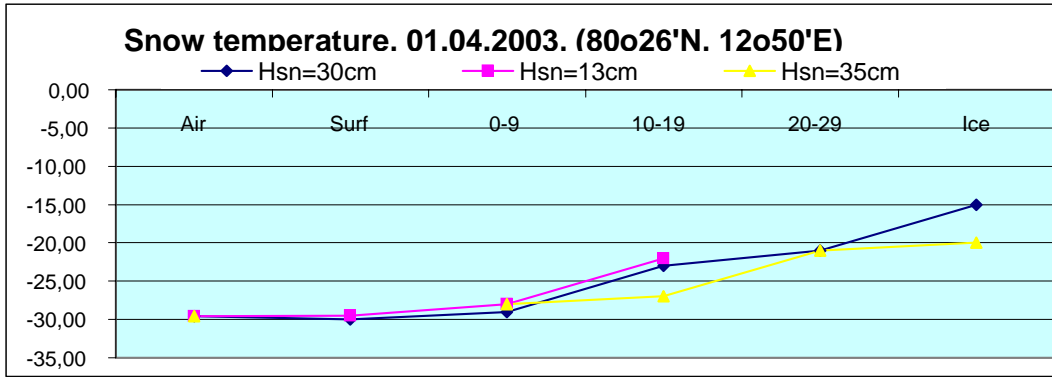
4.2 Snow measurements by NERSC

Several key snow parameters were measured including snow density and depth. These are important for the interpretation of satellite imagery. During the ice stations snow depth was measured randomly on ice floes of different thickness. Temperature/density profiles were obtained in several snow pits using a special snow density kit.

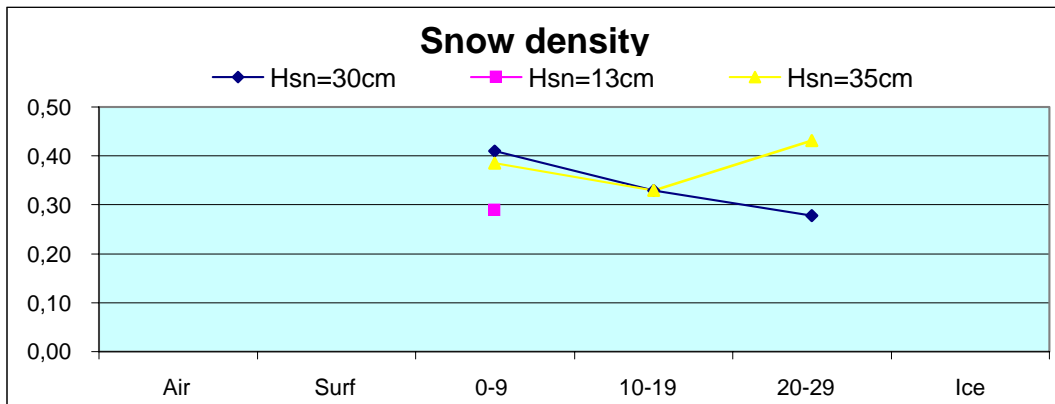
Altogether 41 snow pits were investigated (Table 6). These measurements were conducted on different sea ice types: thin, medium, thick first-year and multiyear ice. The temperature profiles of snow were obtained for different snow depths in the wide band from -1°C to -30°C . Snow measurements were supported with photos of ice floes, snow structure, and upper layer of the snow. Examples of snow profile data are shown in Fig. 24 and summary of the measurements north of Svalbard are shown in Table 7.

Table 6: Summary of snow measurement positions.

N	Date	Coordinates	Number of snow pits	Snow depth	Tair, °C
1	March 7	76° 37'N/17° 57'E	1	Yes	-18.8
2	March 8	76° 35'N/20° 37'E	1	Yes	-13.0
3	March 9	76° 38'N/19° 30'E	1	Yes	-10.7
4	March 10	76° 50'N/19° 02'E	-	Yes	-16.3
5	March 11	76° 50'N/19° 30'E	-	Yes	-26.0
6	March 12	76° 49'N/20° 13'E	2	Yes	-29.0
7	March 16	77° 33'N/20° 21'E	1	Yes	- 9.6
8	March 17	77° 33'N/20° 21'E	3	Yes	- 16.5
9	March 19	77° 17'N/20° 05'E	2	Yes	- 21.8
10	March 21	76° 49'N/19° 23'E	2	Yes	- 4.1
11	March 22	76° 27'N/21° 53'E	2	Yes	-13.8
12	March 23	76° 17'N/23° 22'E	4	Yes	-20.6
13	March 24	75° 58'N/25° 36'E	3	Yes	-19.0
14	March 25	75° 55'N/27° 01'E	1	Yes	-19.0
15	April 1	80° 26'N/12° 50'E	3	Yes	-29.6
16	April 7	81° 54'N/09° 35'E	2	Yes	-21.0; -17.0
17	April 8	81° 54'N/09° 35'E	2	Yes	-17.7; -19.0
18	April 10	81° 49'N/09° 31'E	1	Yes	-20.1
19	April 12	81° 49'N/09° 31'E	3	Yes	- 1.2
20	April 14	81° 49'N/09° 31'E	3	Yes	-7,6; -10.0
21	April 15	81° 47'N/10° 16'E	2	Yes	-13.0
22	April 17	81° 45'N/09° 55'E	2	Yes	-14.9



a



b

Figure 24. Profile of a) snow temperature and b) snow density obtained on 1 April 2003. The results of all snow measurements taken north of Svalbard are shown in Table 7.

Table 7. Snow measurements from the CryoVex study area and calculated ice thickness from freeboard

Date	Time	Latitude	Longitude	Snow depth (cm)	Snow load (Kg/m ²)	Hi F=0.5; i=0.920	Hi F=0.5; i=0.8335
07.04	15.00	81.54	09.35	18	68	3.36	
07.04	15.00	81.54	09.35	22	87	3.18	
08.04	15.00	81.54	09.35	25	96	2.99	
08.04	15.00	81.54	09.35	30	97	2.56	
10.04	10.00	81.49	09.31	10	33	3.76	
12.04	11.00	81.49	09.31	35	129	2.4	
12.04	11.00	81.49	09.31	22	81	3.13	
12.04	16.00	81.49	09.31	20	88	3.36	
14.04	10.00	81.49	09.31	14	53	3.59	
14.04	14.00	81.49	09.31	07	18	3.90	
14.04	17.00	81.49	09.31	45	154	1.74	
15.04	17.00	81.47	10.16	13	53	3.67	
15.04	17.00	81.47	10.16	22	60	2.95	
17.04	11.00	81.45	09.55	10	31	3.75	
17.04	11.00	81.45	09.55	30	123	2.78	
Average				22	78	3.10	1.88

Table 7 also indicates the estimated ice thickness (H_i) using a freeboard (F) of 0.5 m and ice density of MY ice of 920 kgm^{-3} and 833.5 kgm^{-3} . The former value is typical density for MY ice with meltponds, while the latter was observed density in the study area. The two different densities are used to illustrate the sensitivity of the retrieval of ice thickness from freeboard to snow and ice density. The higher density gives a thickness of 3.10 m, while the lower density gives 1.88 m. This sensitivity is further discussed in chapter 6.

5. Processing of D2P level 1b data over sea ice

5.1 Background

This chapter describes the processing of the data from the airborne radar altimeter (D2P) which are similar to SIRAL to be flown on CryoSat. The D2P radar has been used to collect altimeter data over sea ice in 2002 (the LaRA campaign) and 2003 (the CRYOVEX campaign). D2P is acronym for Delay /Doppler Phase monopulse, which is designed by the Johns Hopkins University, Applied Physics Laboratory (JHU-APL). Data and the final report from the LaRA campaign (Raney 2003) is available and have been used in this study.

In both the 2002 and 2003 campaigns, the aircraft carried an optical laser altimeter in addition to the D2P radar to measure the distance to the top of the snow cover. In 2002, the instruments were mounted onboard a NASA P-3 aircraft. In 2003 the instruments were mounted onboard the Danish DNSC aircraft, and the simultaneous laser measurement was made by the DNSC lidar. The 2003 flights were made simultaneous with CRYOVEX'03 expedition with the German icebreaker Polarstern, conducting in-situ observations, and also with satellite imagery from the Envisat ASAR in WS-mode. Processing of a subset of the 2003 laser data and comparison with near-simultaneous ASAR imagery has been made. Also, the effect of snow on the use of altimeter data measuring freeboard, either the snow-freeboard (by laser) or the ice-freeboard (by radar) for ice thickness computation has been investigated and is reported in chapter 6.

In this chapter Level 1b-data from the LaRA campaign in May 2002 field campaign has been investigated for retrieval of height amplitude profiles. Also Level 1b data from April 2003 are available and preliminary processing of these data has been made. Both the 2002 and 2003 data subsets chosen are mainly over the northern sea-ice, at 85.3N, 25W in 2002, and near Polarstern at 82N, 10E in 2003.

5.2 Radar altimeter signal

The D2P radar is a coherent altimeter that operates near 13.9 GHz. The linear FM chirp signal at 5 watts peak power has pulse length selectable in 4 steps from 0.384 to 3.072 microseconds. Over glaciers, two antennas are used to increase the resolution in cross-track. Over sea-ice, only one antenna is used, with doppler history processing made along-track to increase resolution in this direction. Full digital recording of the data is made. The data are available in Level-1 format (file name = D<date>), with each data bloc containing a single radar pulse. These data are the not-dechirped spectra of the 2 channels (antennas). Data are also available in Level-1b, called "processed" format (file name = P<date>). In this case, the data are delay /doppler-processed to an array of calibrated complex cross-channel waveform data. Each sampled waveform has a header giving the time, position, attitude, etc. of the aircraft. The antenna has an 8° cross-track beam width. Along-track, the antenna's 4° beam width is narrowed by the Delay/Doppler processing. Boresight (pointing) was in 2002 found to be about 2.5° off nadir in cross-track, but is precise at nadir along-track.

5.3 Processing of waveforms

In the processed (or level-1b) data, each pulse is a single measurement of the ice, giving signal amplitude (alternatively called magnitude) versus delay (or vertical distance). The complex waveform data found in the P-files are converted to amplitude (and phase if required) using the Fram-fortran program rd2p.f. An example of amplitude versus sample number is shown in Fig. 25a. This signal is from 18 May 2002 over the Greenland ice at 77.082N, 301.15E, found in file P20020518.004, record no 3100. The shown amplitude is in dB, with the peak of 4.27dB located near mid-sample (no.128).

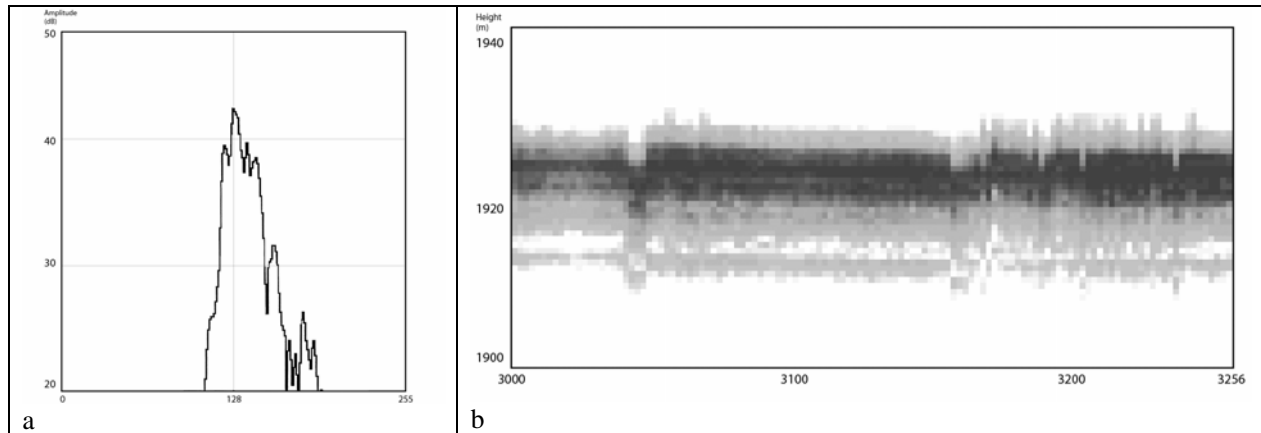


Figure 25. a) Amplitude (in dB) versus sampling number (differential range) over the Greenland ice sheet obtained by the D2P radar on 18 May 2002; b) along-track profile of amplitude in grey-scale (white = 20 dB, black = 50 dB) versus height above the ellipsoide over the Greenland ice sheet at 77.08N and 301.1 E.

5.4 Range calibration and height of signal

The range from aircraft to the ice reflection is stated as the sum of 4 terms: 1) pulse-length, 2) tracking-range, 3) waveform-delay (zero-delay) and 4) calibration-offset. These should give the distance to waveform sample no. 1. Time is given in μs , the corresponding distance in meter is found multiplying by 150 m/ μs (half of the light speed due to 2-way pulses). Reflection height (ice surface height) is then altitude (A/C height above reference height) minus range. Reference height is assumed to be a standard ellipsoide.

An example of processed D2P data from 18 May 2002 is shown in Fig 25 b, where data over Greenland ice sheet are presented (file P20020518.004 rec.no 3100). The data set is characterized by:

- Pulse-length = 230.24 m
- Tracking-range = 1.7987 m x 175 tracking – range steps (from Header) = 314.78 m
- Zero-delay = 0.768 μs /115.2 m
- Calibration-offset =23.98 m
- Altitude = 2496.88 m (from Header)
- Tracking-shift = 9242

Reflection height of the first sample = Altitude - (Pulse length + Tracking range) = 1951.86 m. This value then corresponds to the height of the first waveform sample. In the LaRA report, the length of each waveform of 256 samples is given as 53.3 m. The peak is at sample no. 128 (26.65 m from sample no.1), subtracting this value place the peak power at a height of 1925.21 m, in good correspondence with the LaRA report (Raney and Leuschen, 2003). The equation is therefore (values in meter):

$$\text{Height} = \text{Altitude} - (230.24 + 1.79875 \times \text{Tr.Range} + 0.2082 \times \text{Waveform sample-no.}) \quad (1)$$

Notes:

- The sample-interval of 0.2082 m is not given explicitly in the Raney report.
- Header time and positional data are absent in many of the waveform records.
- The use of the Zero-delay value and the Calibration-offset value is not clear.
- In the Header is also a "Tracking shift", in this example the value is 9242. Multiplying with the same sample-interval as for the waveform gives $0.2082 \times 9272 = 1924.18$ m - very close to the peak power height of 1925.21 m found above.
- In table 6 in the LaRA report, the measured calibration mean difference D2P-GPS =23.974 m, while the text states the value 24.98 m as the correction applied to all processed data.
- Waveform sampling interval in the P-files with 256 samples is 0.2082m (from the figures /waveform-data in the report). In the report however the waveform examples are with 512 samples (0.1m interval). The text also state that the waveforms requires sampling on the order of a few centimeters (the desired precision of measurements).

5.5 Processing to along-track profiles

In order to present the height signal along the flight track, the amplitude in dB is displayed in greytone using equation (1). An example of height versus the waveform-number (that is: along-track distance) in this presentation is shown for the Greenland ice sheet in Fig 25b. The signal starts at 77.085N, 301.117E and ends at 77.082N, 301.160E, a distance of 1150 m Along-track interval is then 4.5 m/sample.

Fig. 26 a and b show examples of amplitude versus sample number over sea ice from 23.May 2002 15:17:06z. This subset is obtained north of Greenland at 85.35N, 335E (file P20020523.012, rec.no. from 24500 to 24756) and shows two typical waveforms, one for rough multiyear ice and one for smooth, thin ice.

An example of along-track profile of amplitude over sea ice using records 24500 - 24756 (file 012 north of Greenland) is shown in Fig. 27.

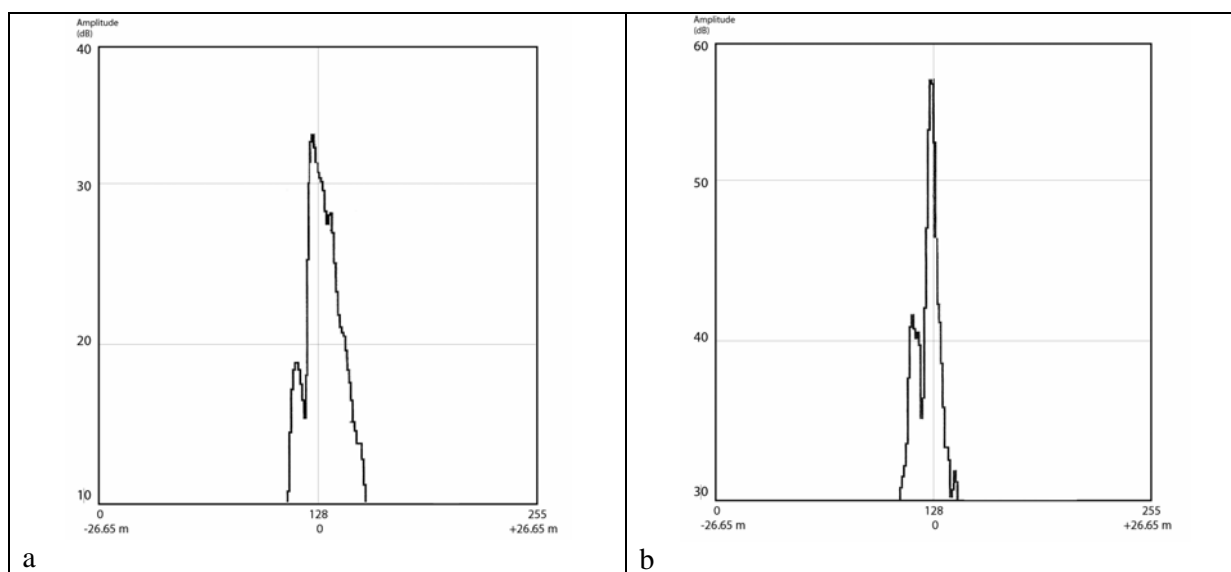


Figure 26. Amplitude versus sample number (differential range) from the D2P radar over sea ice obtained during the LARA campaign on 23 May 2003, file 012. a) record no 24000 from rough multiyear ice, b) record no. 24755 over smooth ice in a lead.

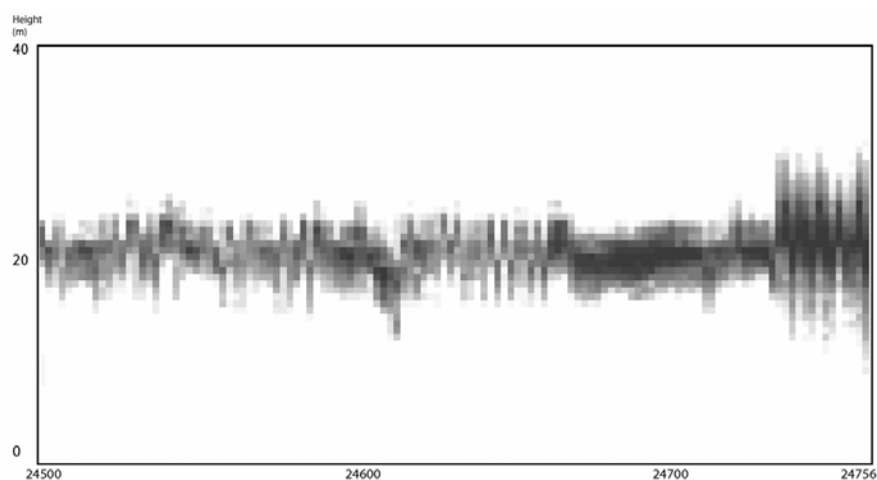


Figure 27. Along-track profiles of amplitude over sea ice presented in grey-scale (white = 20 dB, black = 50 dB) versus height above the ellipsoid north of Greenland at 85.35N, 335E.

5.6 Discussion

The amplitude profiles in Figures 25a and 26 are more noisy than the ones shown in the LaRA report, and have also coarser resolution as noted above. Sudden shifts in the waveform height of about 2 m (10 samples) occurs, the reason is not yet known.

Over the Greenland ice sheet (Fig 25a), the first peak at sample 122 is attributed to the air-snow interface reflection, while the main peak at sample 128 comes from the snow-ice interface. The distance between the two surfaces which is equivalent to the snow thickness, can then be calculated

to be $6 \times 0.2082 \text{ m} = 1.25 \text{ m}$. The peaks on the right side of the maximum are due to reflections at larger depths caused by layers deeper in the ice.

Over the Arctic sea ice the first waveform (Fig. 26a) is assumed to come from the snow surface of rough multiyear ice. The main peak at sample no. 127 is assumed to come from the snow-ice interface. In Fig 26 b, the waveform is from smooth ice in a lead /polynya. The reflection is much stronger than over multiyear ice (+2.3 dB) and the signal is also much narrower (specular reflection versus diffuse reflection). The air-snow interface reflection is not seen here.

This procedure in this chapter describes how level 1b data from a Delayed Doppler Radar (D2P), which is similar to SIRAL on CryoSat, is processed to give height-calibrated amplitude profiles (level 2 data) which are used to calculate freeboard and retrieve ice thickness from radar altimeter.

Further examples of D2P along-track profiles from the Cryovex campaign are shown chapter 6.

6. Synthesis of results

In this chapter the different observation methods used in CryoVex 2003, presented in chapters 2 – 5, are compared and results of the measurements are presented and discussed in the context of validating CryoSat data for ice thickness retrieval.

The *in situ* measurements of snow and ice parameters have been compared with freeboard and thickness measurements obtained by the airborne laser scanner and the EM-bird. SAR images were geolocated with the various other data sets for determination of thin and thick ice, leads, ridge areas and large MY floes. The most important dates for comparison of the different observign systems were 11 and 15 April. A few D2P profiles have been obtained, but all the processed D2P data from CryoVex have not been included in the study so far. Comparison between EM, airborne laser scanner and ground-based EM sensors have been presented in Chapter 3.

6.1 Comparisons on 11 April

The first coincident aircraft laser and D2P survey and HEM flight was performed along a transect from the Polarstern location (point A in Fig. 28a) to point B 100 km to the southwest. The SAR image (Fig 28a) shows the ice conditions in the area with the flight line superimposed. The laser profile from point A to B is shown in Fig. 28b, indicating that the average freeboard over the distance A – B is 0.55 m. The variability in freeboard is significant, varying from about 1.2 m for the ridges north of the MY floe to less than 0.20 m in the leads. The co-location of the two data sets confirms that areas of thin ice or open water between ice floes in the SAR image have a surface height between 0 and 20 cm. The MY ice which constitutes most of the laser profile, has most of the freeboard measurements between 0.39 and 0.65 m (Fig. 29).

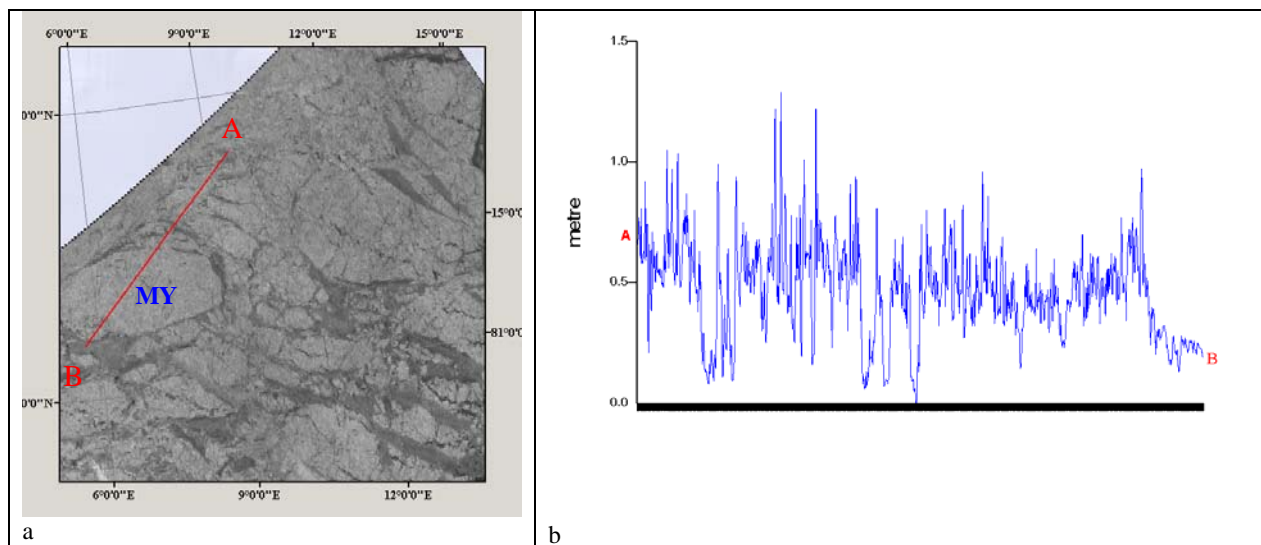


Figure 28. a) Subset of an ASAR widesswath showing the location of the scanning laser profile starting from the location of Polarstern (point A) and extending in a southwesterly direction to point B; b) the laser profile showing surface height above sea level.

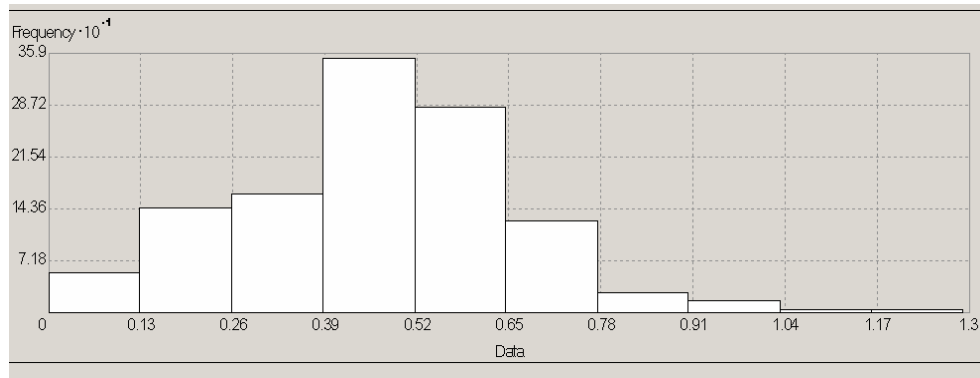


Figure 29. Histogram of the laser profile data in Fig. 28 b.

An example of comparison of ASAR classified sub-image, laser scanner data and video images from 11 April 2003 is shown in Figure 30. The laser scanner data shows good capability to distinguish between multiyear ice (higher freeboard) and thin ice (lower freeboard) as shown in Fig 30 b. This is confirmed by the SAR classified image derived from alternating polarized images (Fig 30 a). Comparison between laser data and vertical photographs have been done for several test areas. For example, leads, ridges and floes can easily be identified in the photographs and collocated with height measurements from the laser, as shown in Figure 30 c.

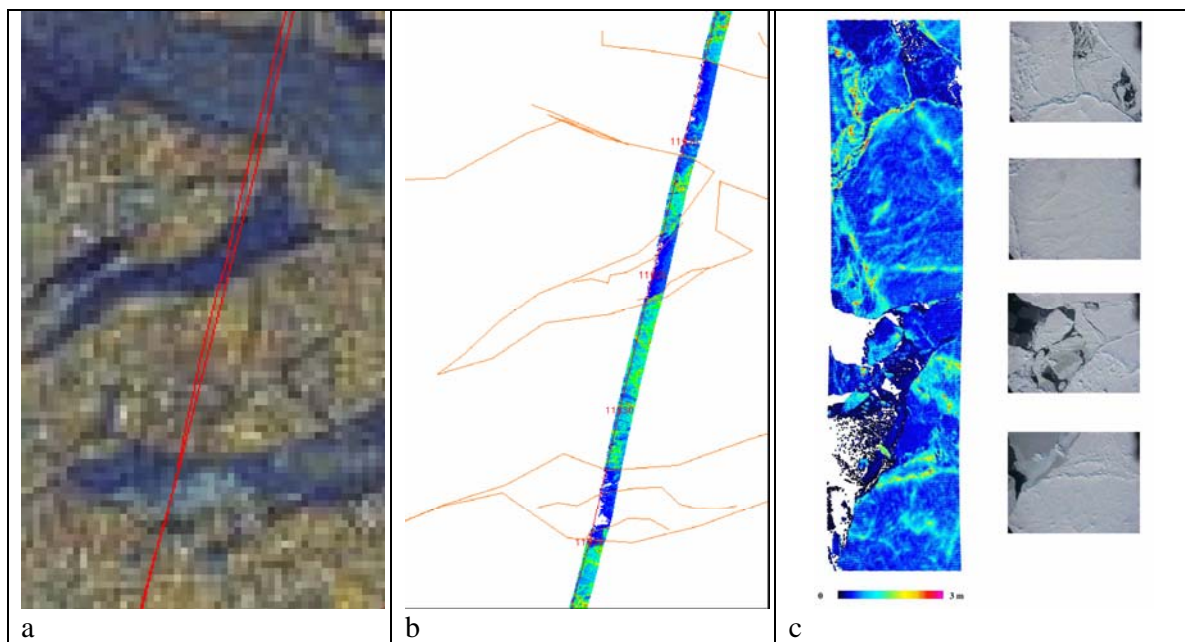


Figure 30. a) ASAR ice classification from alternating polarisation imagery on 11 April 2003, with the laser flight line superimposed. The brownish signature indicates multiyear ice, while blue indicates thin ice; b) the scanning laser data showing that the low freeboard (blue signature) corresponds to the thin ice and the high freeboard (green signature) corresponds to the thick multiyear ice. The swath width of the laser data is about 300 m and the length of the images are about 10 km. The time difference between the two data sets were about 30 minutes. C) shows a comparison between scanning laser data and co-located vertical photographs from another flight line obtained in 2003.

6.2 Comparisons on 15 April

The second long transect of simultaneous airborne laser and D2P profiles with EM data was obtained on 15 April in the area north of Polarstern. The SAR image with the transect superimposed is shown in Fig. 31, where Polarstern is located at point A. The ice conditions along the transect is very homogeneous, consisting of multiyear ice with scattered small leads appearing as dark line features in the SAR image. The collocated laser and EM profiles of freeboard measurements for the 100 km transect is shown in Fig. 31 b, indicating fairly good match between the two data sets.

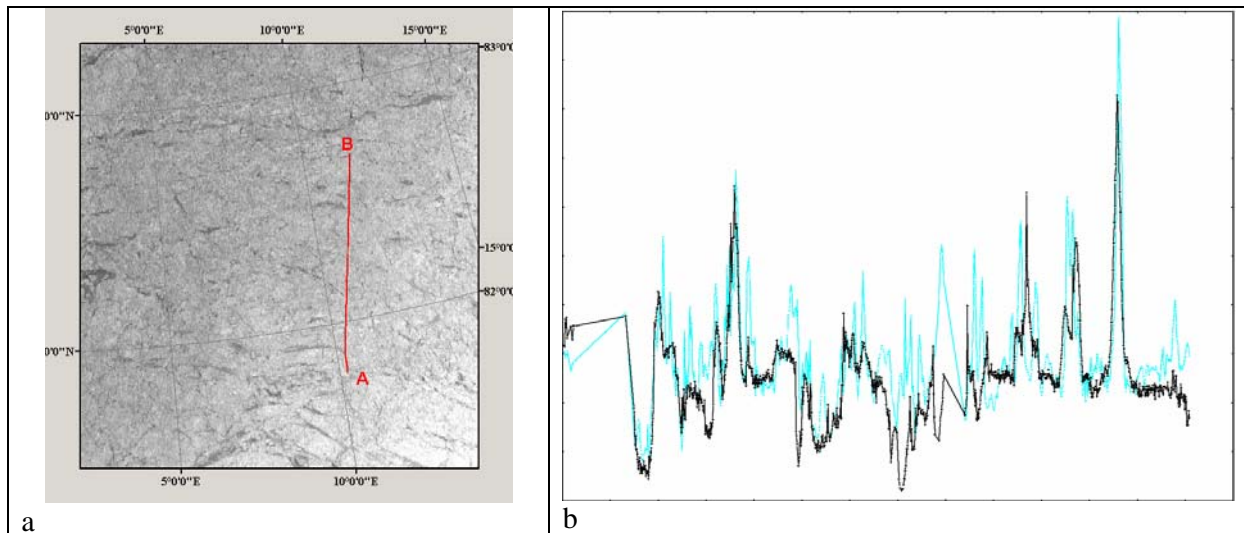


Figure 31. a) Subset of SAR image with the flight track for 15 April superimposed. The location of Polarstern is near point A; b) profiles of laser freeboard (black) and collocated EM freeboard (blue) for the 100 km track.

By matching the thickness distributions from the two data sets, assuming that the EM data provides the “true” thickness measurements, the sea ice density can be estimated to be about 850 kg/m^3 . This assumes that snow parameters are known. Further discussion of this method of ice thickness retrieval is presented in section 6.3.

One example of ice thickness retrieval from freeboard observed by the D2P radar is presented in Fig. 32, where a small part of the 100 km track is plotted both from the D2P. The D2P profile, indicated by the colour scale, shows the along track profile of amplitude as function of ellipsoid height (similar to the plots in Fig. 25b and 27) for a distance of about 2.5 km. The laser profile is shown as white dots. The D2P and laser profiles agree well to observe peaks and troughs of the ice surface. It is noteworthy that the laser profile are typically 30 cm higher than the maximum amplitude of the D2P data. This is in agreement with the assumption that the D2P data penetrate the snow cover, while the laser data are reflected at the top of the snow layer.

A “calibration flight line” for the D2P was obtained on 11 April when the Twin Otter flew from Longyearbyen over Isfjorden where the ice-cover was undeformed and thin. This allowed for a comparison between D2P and laser profiles over a homogeneous, flat ice surface, as shown in Fig. 33.

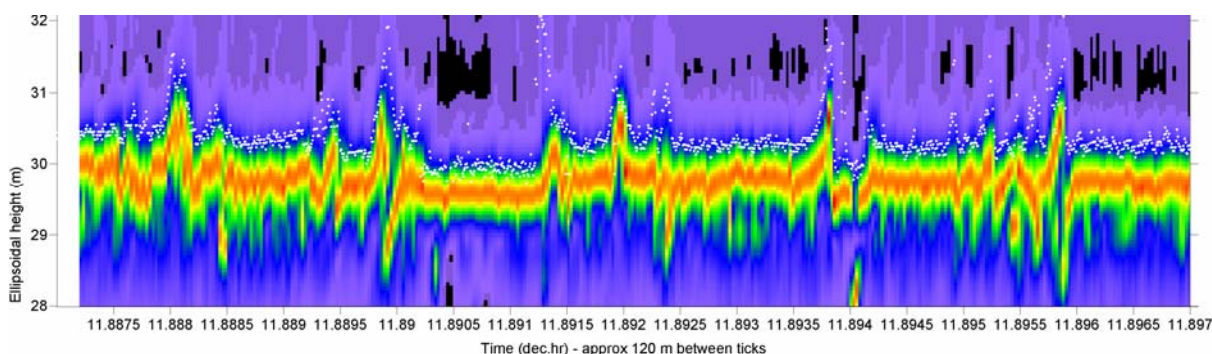


Figure 32. D2P measurements of ice surface height shown in colours where the orange represent maximum amplitude. The scanning laser data are shown by the white dots. The length of the profile is about 2.5 km.

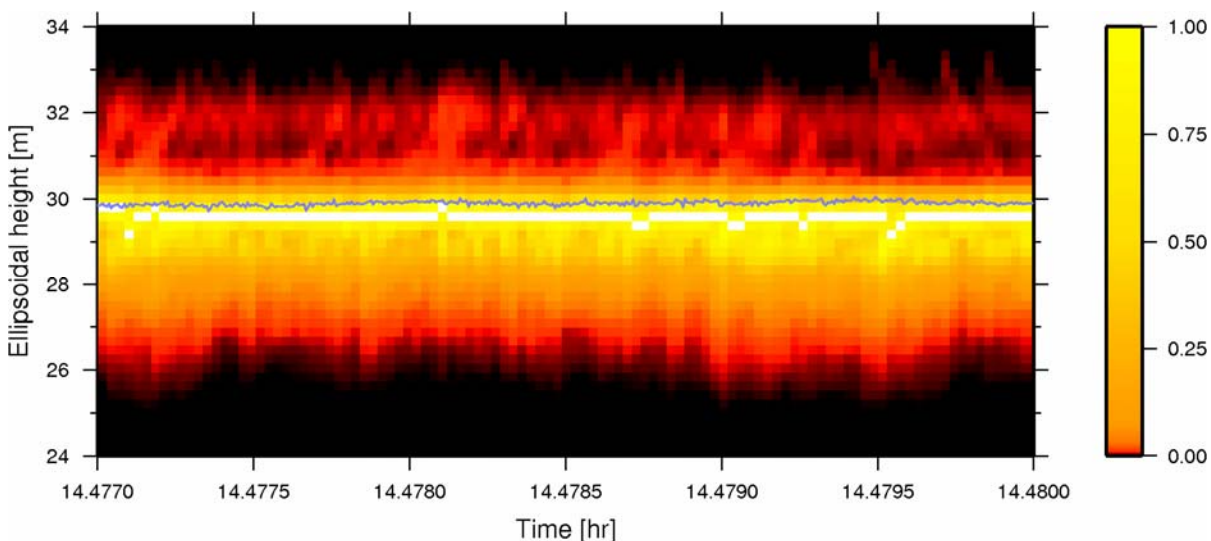


Figure 33. Excerpt of the D2P “ calibration flight” over Isfjorden when flying from Longyearbyen to the Poølarstern area on 11 April. Maximum amplitude of the D2P data are shown by the white line, while the laser profile is indicated by the grey line. A small difference between the two profiles (10 – 20 cm) can be explained by the snow cover on top of the ice.

6.3 Calculation and direct measurement of ice thickness

Calculation of ice thickness from freeboard measurements, supported by in situ snow and ice measurements, depend on how representative the measurements are, and to what extent there are enough data do show the typical variability of the snow and ice properties in the study area. For this purpose we have compared estimates fro CryoVex with statistics from literature based on Russian surveys of the Arctic sea ice over many years.

Statistics of snow and ice parameters for the whole Arctic has been compiled by Russian surveys over many years, and have been published in various reports and in the atlas by Romanov (1995). Ice density is one of the most sensitive parameters in calculation of thickness from freeboard measurements. This is illustrated in Table 8, where typical range in ice densities shows the impact on the thickness calculation. For multiyear ice, the density varies typically between 820 kg/m^3 to 920 kg/m^3 , giving a range in ice thickness between 1.76 m to 3.39 m. The lower densities are found in MY ice with hummocks where more air pockets are embedded in the ice. The higher values are

found in MY ice with melt ponds, where the freshwater content brings up the density. Direct measurements of ice density in the CryoVex area showed values of 833 kg/m^3 and 836 kg/m^3 .

Table 8. Ice thickness as function of ice density (from Romanov, 1995).

Ice density $\text{kg/m}^3 \times 10^{-3}$	0.78	0.80	0.82	0.84	0.86	0.88	0.90	0.92	0.94
Hi (m)	1.48	1.60	1.76	1.95	2.18	2.47	2.86	3.39	4.16

The snow distribution on sea ice is very variable and existing data and statistics of snow on ice are scattered in space and time. The most extensive analysis on snow climatology in the Arctic is produced by Warren et al (1999), but Warren's study which is based on data from all the North Pole drifting stations has no data for the area north of Svalbard. Romanov (1995) has produced statistics of snow parameters for the whole Arctic including the Fram Strait area based on aircraft surveys and landings over many years. Statistics of snow parameters in the CryoVex area from Romanov (1995) is shown in Table 9.

Table 9. Snow depth statistics for the month of April in the CryoVex area.

Snow properties	Minimum	Average	Maximum
Level ice	25 cm	35 cm	45 cm
Ridges	40 cm	100 cm	150 cm
Snow tongues (snow height and length)	45 cm / 15 m	70 cm / 30 m	100 cm / 45 m
Sastrugi (snow depth and area in %)	40 cm / 40 %	55 cm / 50 %	60 cm / 70 %
Ice thickness	150 cm	240 cm	300 cm
FY ice area (%)	15 %	40 %	70 %

Calculation of ice thickness from measured snow and ice properties is done as follows for three cases north of Svalbard where MY ice dominates:

1. Profile obtained from laser altimeter on 11 April southwestwards from Polarstern (Fig. 28)

Freeboard (snow + ice) for MY ice from the long laser profile 0.55m on average

Snow depth = 22 cm (mean value from in situ measurements in Table 7)

Snow load = 78 kg/m^2 , giving snow density of 360 kg/m^3

Water density = 1028 kg/m^3

Result: ice thickness is estimated to be

3.5 m for $\rho_i=910 \text{ kg/m}^3$ (assuming a high value of ice density, where many meltponds occur)

or 2.2 m for $\rho_i = 836 \text{ kg/m}^3$ (assuming a mean ice density observed in the study area)

2. Dense survey around Polarstern

Freeboard (snow + ice) for MY ice: $0.65 \text{ m} \pm 0.2 \text{ m}$

Similar data for snow load and water density as from case 1

Result: ice thickness is estimated to be

4.4 m for $\rho_i=910 \text{ kg/m}^3$ (assuming a high value of ice density, where many meltponds occur)

or 2.7 m for $\rho_i = 836 \text{ kg/m}^3$ (assuming a mean ice density observed in the study area)

In this case we can compare the estimated ice thickness with direct observation of thickness:

EM profiles: $2.06 \pm 0.17 \text{ m}$ (thickness of snow + ice)

Drilling holes: 2.38 m (thickness of snow + ice)

Conclusion of the comparison in Case 1 and 2: The real ice thickness is closer to 2.0 m if we take in to account that the direct measurements also include the snow layer which was 0.22 m on average. This suggests that the ice density value to be used in the calculation should be lower than 836 kg/m^3 . In the literature values down to 820 kg/m^3 are reported for MY ice with hummocks.

3. Profile obtained from D2P altimeter on 15 April north of Polarstern (Fig. 31 and 32)

An example of ice thickness calculation based on freeboard data from D2P is presented in this paragraph. The example is taken north of Polarstern on 15 April. Snow data are taken from the statistics by Romanov (1995) since no in situ measurements were obtained in this region. The freeboard data from D2P is for ice only, where the mean estimate for the section shown in Fig. 31 is 0.30 m. The ice type is mainly MY ice as observed in the SAR image. The snow depth is on average 35 cm using the Romanov data. Snow density is assumed to be 360 kg/m^3 , the water density 1028 kg/m^3 . Calculation of ice thickness based on these input data gives 3.1 m using an ice density of 887 kg/m^3 . The sensitivity to the snow layer can be estimated as follows: assuming that snow thickness has a std of $\pm 0.10 \text{ cm}$, it will lead to a std of $\pm 0.26 \text{ cm}$ in ice thickness. The largest uncertainty, however, is in the density of sea ice.

6.4 Ice thickness synthesis maps from airborne and satellite laser data

DNESC has compiled ice thickness estimates from all the airborne surveys carried out north of Greenland and in the Fram Strait region in May 2002 and April 2003 and presented in Fig. 34.

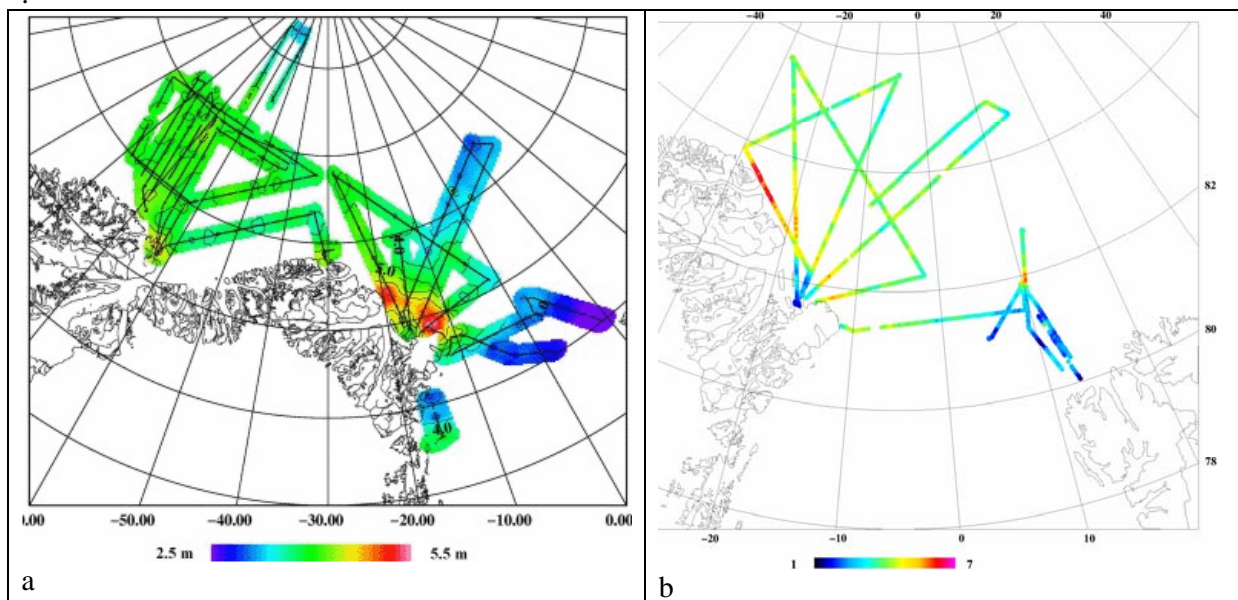


Figure 34. Flight lines and corresponding thickness estimates from airborne laser and GPS measurements performed by DNESC in 2002 (a) and 2003 (b). Note that the thickness scale is different in the two years.

As discussed before, the translation of freeboard measurements to ice thickness is sensitive to snow and ice density, and we have shown that small variability in ice density can give large variability in ice thickness. The maps in Figure 34 shows features of the thickness distribution which are expected such as accumulation of thicker ice along the north coast of Greenland and thinner ice in the marginal ice zone north of Svalbard.

In March 2003, the first data set from IceSat over sea ice areas was obtained and the first results of the data analysis has been published (Kwok et al., 2004). IceSat, which was launched in December 2003, carries a laser altimeter to measure ice, cloud and land elevation (<http://icesat.gsfc.nasa.gov>). Surface roughness and sea ice freeboard are some of the sea ice parameters that IceSat can measure, and the first data sets were obtained within a month of the CryoVax experiment. Two maps of Arctic surface roughness from IceSat have been published by R. Kwok (Fig. 35), showing that the highest roughness is found north of Greenland and in the Canadian Arctic, while the lowest roughness is found in the areas of firstyear ice. Further comparison and analysis of the data sets from IceSat and from the CryoVax experiment will be needed.

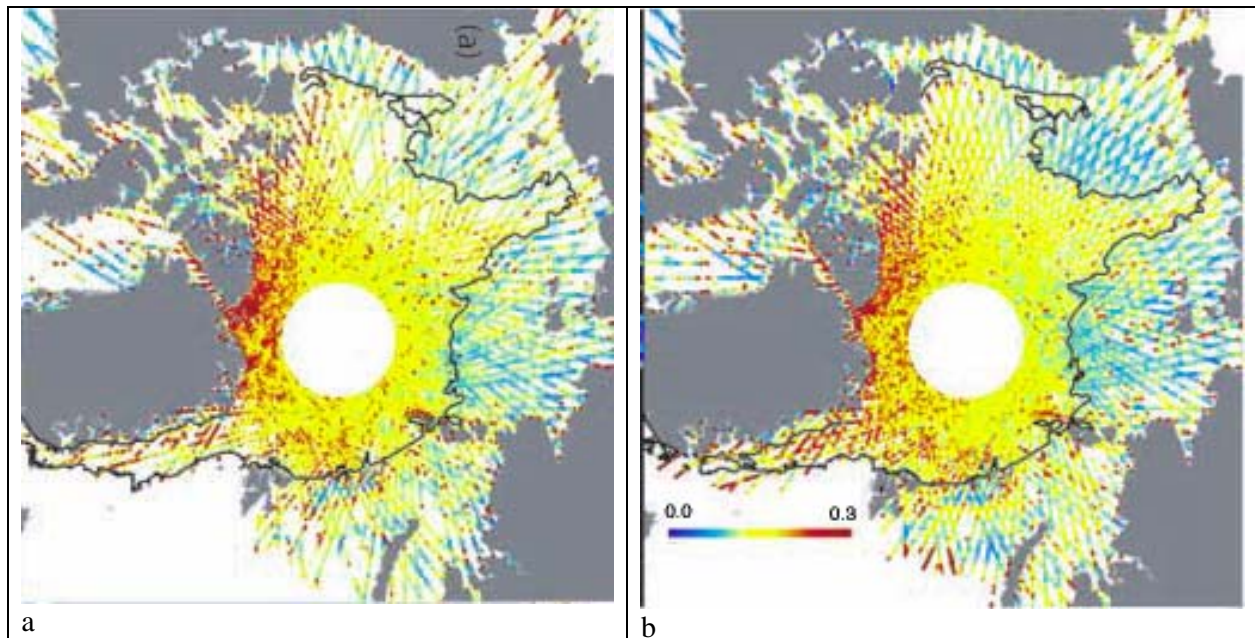


Figure 35. Tracks of IceSat surface roughness at a 10 km length scale (shown by the colour bar) are presented together with the boundary of perennial ice zone (grey line) derived from Quikscat backscatter data for the periods 04 – 11 March 2003 (a) and 12 – 20 March 2003 (b). From Kwok et al., 2004.

IceSat will be a complementary satellite to CryoSat, because laser and radar altimeters measure different properties of the ice surface. The laser signal will be reflected from the snow surface while the radar signal will penetrate dry snow and be reflected from the ice surface, which has been documented in Fig. 26, 32 and 33. The thickness of the snow layer on top of the sea ice can in principle be estimated by combining laser and radar altimeter data. The spatial resolution of the IceSat laser data is higher than the CryoSat radar data, about 70 m, compared to 250 m for the radar data. IceSat will also provide limited temporal coverage because of limitation due to light and cloud conditions, while CryoSat will provide good data year round.

7. Results of pre-launch sea ice cal/val activities at Norwegian Polar Institute

7.1 Overview

The Fram Strait is a key area for studying Arctic sea ice mass balance, ice dynamics and freshwater balance. Most of the multiyear ice that is transported with the transpolar drift exits the central Arctic Ocean through the Fram Strait. The Norwegian Polar Institute (NPI) has conducted continuous Fram Strait sea ice monitoring since the beginning of the 1990s, based on moorings placed in the western part of the Fram Strait (Vinje et al. 1998; Vinje et al. 2002, Hansen et al. 2004, see map in Fig. 36). Since 2003, those measurements are supplemented with regular in situ sea campaigns during September using the NPI research vessel “Lance” (Hansen et al. 2004, Gerland et al. 2005; see also Sandven et al. 2005). This will be continued in 2005, with an additional large-scale expedition will investigate the Fram Strait during May and June, and with the regular R/V Lance cruise in September. Mooring measurements include temperature and salinity monitoring, current speed and ice draft (upward looking sonar “ULS”). Usually, four NPI-ULS sensors are installed in the Western Fram Strait in the area, where most of the multiyear sea ice exits the central Arctic Ocean.

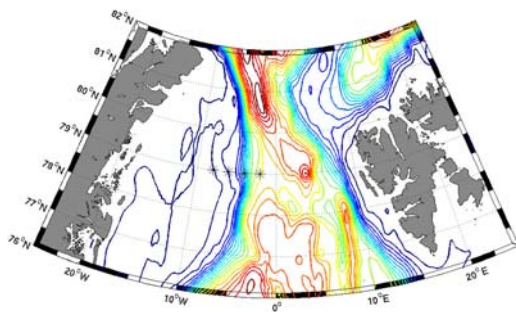
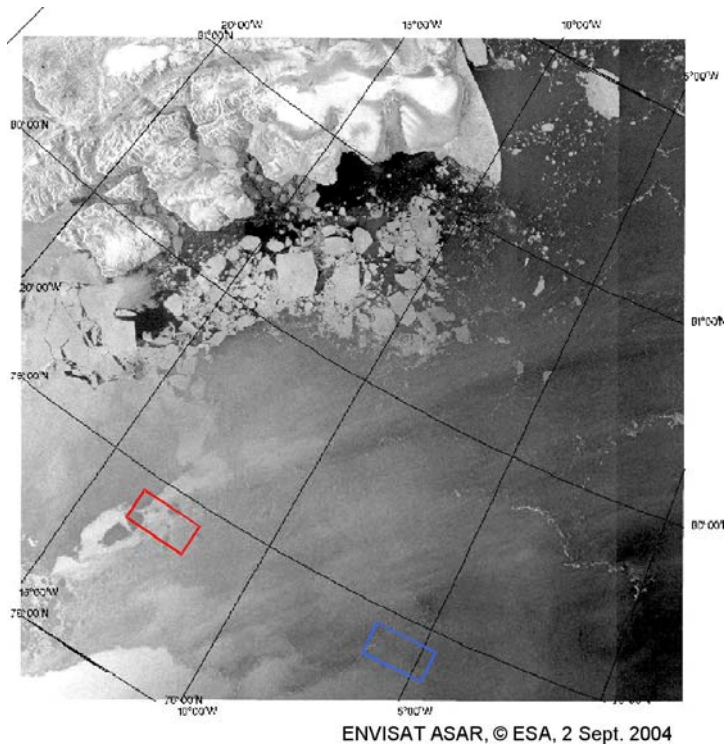


Figure 36 (above) Map of the Fram Strait with the east coast of Northern Greenland in the west and the Svalbard archipelago in the east. The NPI mooring positions with upward looking sonars are marked by stars.

Figure 37 (right) The western Fram Strait with the research areas for the 2003 in situ fieldwork (blue rectangle) and for 2004 (red rectangle). The 2004 in situ stations were located west of the ULS mooring positions because of lack of ice in the region where the moorings are located.



The techniques employed during the regular in situ campaigns have been successfully applied by NPI researchers to various studies in the Barents Sea and Svalbard fjords (e.g. Gerland et al. 1999).

7.2 In Situ Measurement techniques

Observations techniques include snow and ice thickness measurements by both drilling/sounding and electromagnetic profiling (using a Geonics EM31; see e.g. Haas et al. 1997), measurement of physical snow properties (density, temperature, salinity, moisture, stratigraphy, classification, grain sizes) and optical surface properties (spectral albedo and reflectance). From 2004 onwards, in addition to the in situ measurements, a monitoring camera for ice concentration and type detection is installed on RV Lance. This system, called IceCam (see Hall et al. 2002), registers ship navigation data along with a digital image of the view to the ice surface from the bridge, and along with meteorological data measured by the ship's weather station. In 2004, a set of ENVISAT SAR images could be obtained simultaneously to the in situ fieldwork. This was possible because of support through an ESA CryoSat Data AO project # 2669 with the title: "Combined sea ice thickness investigation using CryoSat, upward looking sonar and in situ observations", (PI: S. Gerland).

7.3 Selected results

The specific working areas were different for the 2003 and 2004 fieldwork. In September 2004, no sufficient sea ice suitable for in situ studies was found in the area where the ULS moorings are installed, and the work was performed further west (see Fig. 37).

September 2003: On 6 ice stations, small multi-year ice floes (range: 50 m diameter) were met, and in total 14 thickness drillings gave direct measured ice thicknesses between 1.90 and >11 m. These measurements were used to calibrate the empirical relation between apparent electrical conductivity and ice thickness, necessary for the processing of electromagnetic measurements. 6 profiles with electromagnetic measurements, total length 365 m, were obtained. The freeboard measured was between 17 and 43 cm, with a mean of 28 cm (13 measurements). Surface water salinity was measured next to the ice floe edges 27.0-30.8 ppt, showing the influence by ice melting.

September 2004: On 8 ice stations, multi-year ice floes on average bigger than in 2003, were investigated with usually two electromagnetic profiles (14 profiles with 960 m length in total), calibration drillings (16 in total), and measurements of physical properties of snow. ENVISAT ASAR WS (8) and NS/AP (5) images were obtained parallel to the fieldwork

7.3.1 Ice and snow thickness

Ice thickness was measured both directly in drill holes and indirectly with an electromagnetic device (Geonics EM31) along profiles. The direct measurements give also freeboard information, whereas the electromagnetic measurements results in data for total ice thickness (snow and ice); snow thickness was measured parallel to each electromagnetic measurement.

The ice floes observed in 2003 exhibited some relatively thick multiyear ice. Since the floes were at the same time relatively small, it seems that the ice consisted besides of regular multiyear ice to some degree of old ridges/hummocks. In contrast, in 2004, larger ice floes could be investigated, and the thickness distribution (Fig. 38b) resembles more those distributions known from other investigations over Arctic multiyear ice (e.g. Haas 2004).

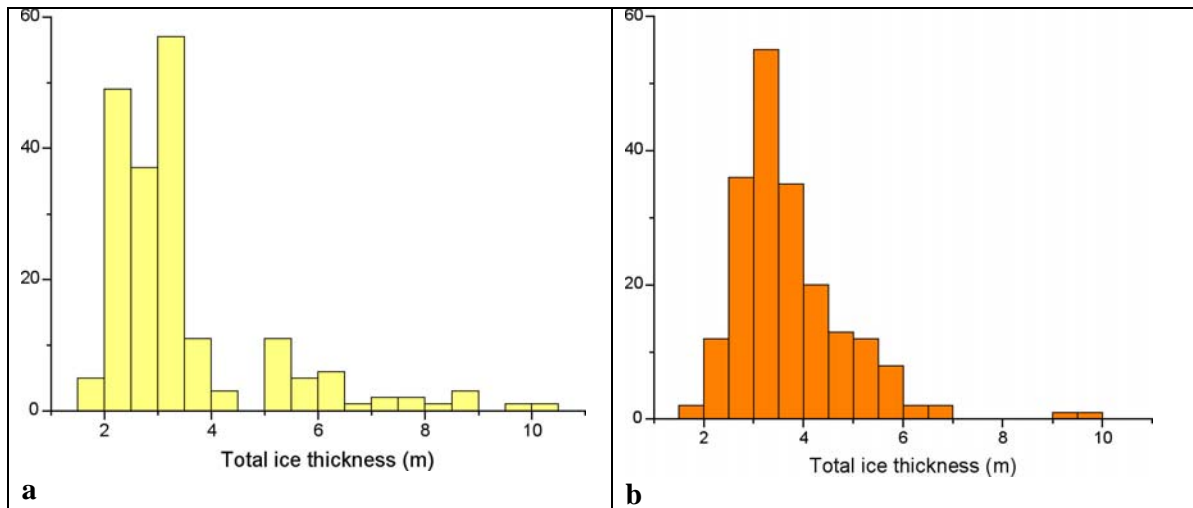


Figure 38. Histogram of total ice thickness from electromagnetic measurements in a) September 2003, and b) September 2004.

Snow thickness sounding resulted in substantial different snow thickness distributions for September 2003 and 2004. In 2003, the snow cover was always less or equal 4 cm thick (usually between 0 and 1.5 cm), consisting of snow with rounded grains/faceted crystals usually 0.5-1 mm (max. 2 mm) large. In 2004, the average snow thickness was larger than for 2003, usually round snow grains 0.5 – 2 mm diameter, often frozen together to larger pieces of crusts (types II-B-2, IV-A, IV-B, after LaChapelle 1992).

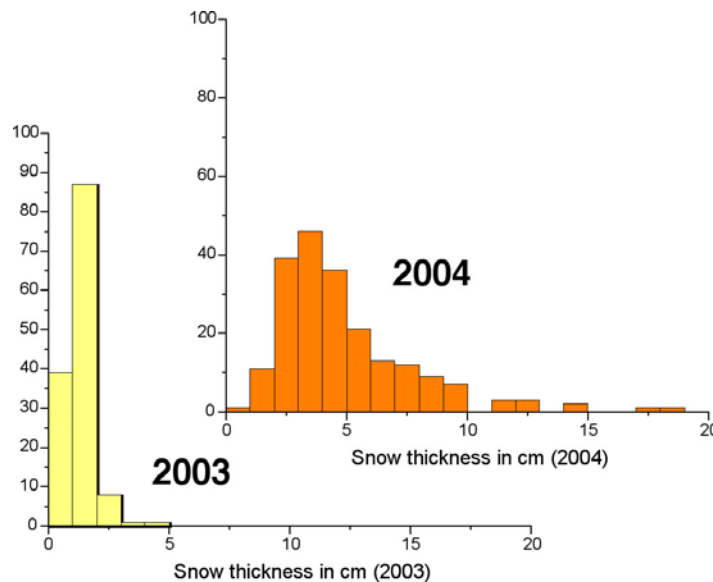


Figure 39: Snow thickness distribution for both campaigns: 2003 (left) and 2004 (right).

7.3.2 Snow density

Snow density was only measured in 2004. Measurements are done while using a half-litre tube which is gently pushed horizontally in the snow, after preparing a vertical snow face in a snow "pit". In total, 8 measurements were applied, resulting in an average density of 390 kg m⁻³ (min: 330, max: 450). Knowing that this is only a small amount of data, it is mentioned here, since density data on snow on sea ice are sparse, and they are crucial for ice thickness calculations when using freeboard or draft data.

7.4 From freeboard/draft to ice thickness

The 16 drillings applied in 2004, mainly for the calibration of the electromagnetic measurements, were used to calculate ice thickness from freeboard and draft measurements, in order to be able to compare those results with direct measurements. The following relations were used for the calculations, following classical hydrostatics and using fixed values for water, ice and snow densities (see Figure 3):

Ice thickness from freeboard (CryoSat principle):

$$h_i = (\rho_w h_f + \rho_s h_s) / (\rho_w - \rho_i)$$

Ice thickness from draft (ULS principle):

$$h_i = (\rho_w d - \rho_s h_s) / (\rho_i)$$

where

d: draft (measured);

ρ_w = water density = 1028 kg m⁻³;

ρ_i = ice density = 900 kg m⁻³;

ρ_s = snow density = 390 kg m⁻³ (mean of 2004 measurements);

h_s = snow thickness (measured);

h_i = ice thickness;

h_f = freeboard (measured).

The upper graph in Fig. 40 shows measured draft and freeboard in drill holes (diameter 5 cm), whereas the lower graph shows the calculated and the measured ice thickness. The different drill locations are not from one single profile, but they are plotted together for practical reasons. The calculations show that methods with relatively small footprints might be influenced by errors related to the non-rectangular cross section of an ice floe, especially when using freeboard. This is important when using high resolution methods for calibration and validation of CryoSat. As an example, drill hole #1 was located in a relative depression, resulting in a small freeboard value, despite an ice thickness of about 6 m. It is obvious that on that basis the ice thickness cannot be calculated from such a single spot. On the other hand, when averaging over larger areas/distances, those errors can be expected to be small. In general, the errors when calculating ice thickness from freeboard were significantly larger than when calculating from draft measurements, as one would expect.

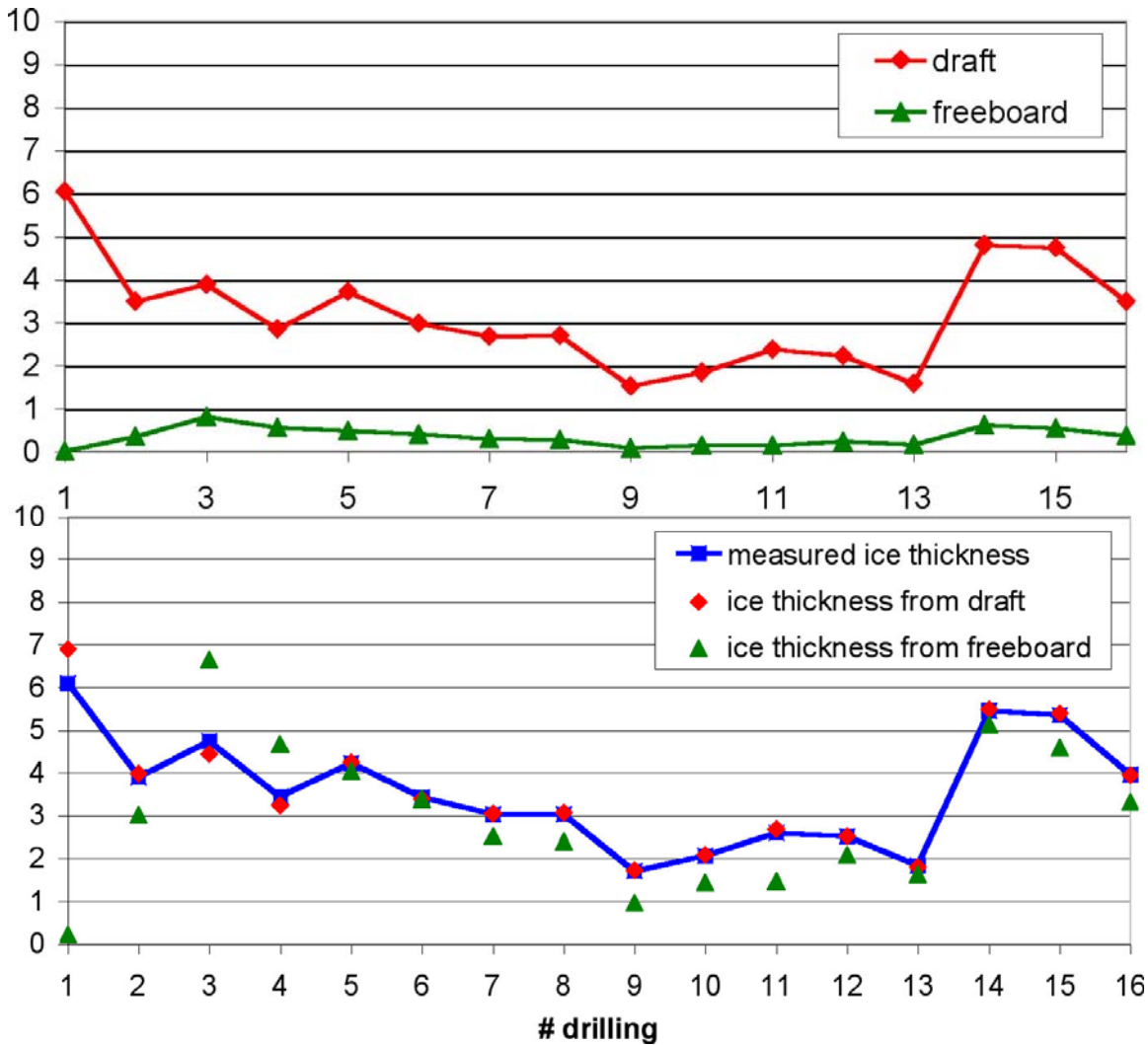


Figure 40: Directly measured freeboard and draft from drill holes on different ice stations, measured in September 2004 (upper panel). Ice thickness from measurements (blue) and calculations (red and green).

7.5 Outlook

The in situ data from surface measurements will be combined with upward looking sonar time series of ice draft for the western Fram Strait once the ULS data processing is completed. Additional data of snow properties, combined snow/ice thickness and freeboard draft measurements from Kongsfjorden with level ice and the Russian NP-33 drifting station (NPI-AARI cooperation) will be used to work in more detail on the investigation of processing issues related to CryoSat altimetry data.

Data from 2005 field campaigns will be added to the existing database. Acquired remote sensing images (ENVISAT ASAR) will support the processing and interpretation of both in situ field measurements and data from ULS.

8. Concluding remarks and plans for further work

This report provides an overview of snow and ice measurements from several field experiments providing useful data for CryoSat pre-launch studies related to sea ice thickness. The most extensive experiments were performed during the Polarstern cruises in the Barents Sea / Storfjorden area in March 2003 and in the area north of Svalbard in April 2003 (also called CryoVex). In addition, summer experiments were conducted during expeditions with the Lance in the Fram Strait in 2003 and 2004. The experiment used a number of different observing techniques from satellites, aircraft, helicopter and in situ observing systems. Several new and unique measurements techniques for sea ice properties were tested and used in combination with established methods. Comparison of methods used simultaneously over the same area is an important part of the work because more established methods can be used to validate new methods. For example, use of the helicopter EM system which has been developed over many years, was successfully used to validate the airborne laser-derived thickness estimates. In situ measurements obtained by drilling holes and using ground penetrating radar give detailed data on local scale. But spatial coverage of these data is very limited and it is challenge to obtain representative measurements for large parts of the Arctic sea ice.

The main results of the thickness measurements in the CryoVex experiment was that in the multiyear floe near Polarstern the mean thickness derived from drilling holes was about 2.6 m with 10 % std. The airborne scanning laser measurements showed a mean thickness of about 3.2 m with up to 20 % std. The laser measurements depend very much on the k-factor which translates freeboard in to thickness. The overestimation by the laser data suggests that the k-factor was too high. In the two 100 km long flight tracks, the scanning laser measurements were compared with helicopter EM data. The track in southwesterly direction showed a mean thickness of about 2.1 m for both systems. The std was up to 71 %, indicating that the variability in ice thickness was much larger for a 100 km long track compared to the measurements on a single floe near the Polarstern. The northward track showed a mean thickness of about 3.7 m in the laser data (std = 46 %) and 3.4 m in the helicopter EM data (std = 42%). The overall result was that the most reliable methods (drilling and EM data) showed a general increase in the mean thickness from south to north over a 200 km distance. The scanning laser data showed larger variability and a tendency to overestimate the thickness in the middle and northern part of the study area. This shows that a constant k-factor for the laser data should not be applied over the whole study area. In future use of laser data, the k-factor should be adapted to the local ice conditions, taking into account that ice density and snow depth vary within a distance of 200 km.

The experiments have provided useful data sets for validation of sea ice thickness data from the upcoming CryoSat. The D2P radar measurements, obtained from the Twin Otter aircraft flights, are similar data as CryoSat will deliver. The analysis of the D2P data, and comparison of the D2P data with the other measurement techniques, is a major objective of the pre-launch cal-val studies. However, only a very limited part of the D2P data, processed to level 2, have been available for this study. The first comparisons between D2P-derived and laser-derived height profiles suggest good agreement, but with a systematic offset where the laser measurements are 10 – 30 cm higher than the D2P measurements. This is expected because the hypothesis is that the radar data is reflected at the snow-ice interface, while the laser is reflected at the top of the snow layer. This hypothesis needs to be further investigated because microwaves in Ku-band (around 13Ghz) can penetrate into sea ice depending on salinity and temperature in the upper part of the ice. An error in freeboard

height measurement of for example 10 cm is magnified to an error of 50 – 80 cm in thickness estimates. Other important problems to investigate are ice density and snow thickness. The ice density is the most critical factor for the thickness determination. Another hypothesis to be further investigated is the isostatic equilibrium for ice floating on water, and the scale where this assumption can be applied.

A major challenge is to obtain validation data covering different areas and seasons. The studies described in this report only provide data from very limited areas, and it is evident that more data of the kind that CryoVex provided is needed in different parts of the Arctic. This should be taken into account in future field experiments in the Arctic. The International Polar Year 2007 – 2008 will offer good possibilities to carry out field investigations across the Arctic Ocean. This will be a good opportunity to collect representative data on snow and ice physics needed for post-launch cal- val studies for CryoSat.

This report only gives a brief overview of the field experiments carried out in 2003 – 2004 and some initial results. More detailed analysis of all the data is in progress and publication of results are expected in near future. The experiments were supported from ESA, several EU projects (SITHOS, GreenICE) and national funding from the participating institutions in Denmark, Germany, Norway and UK.

9. References

- Bourke R.H., Paquette R.G. – Estimating the thickness of sea ice//J. Of Geophys. Res., 1989, vol. 94, N C-1, pp. 919-923.
- Gerland, S., Winther, J.-G., Ørbæk, J.B. & Ivanov, B.V. 1999: Physical properties, spectral reflectance and thickness development of first year fast ice in Kongsfjorden, Svalbard. *Polar Research* 18 (2), 275-282.
- Gerland, S., Hall, R., Hansen, E. & Løyning, T.B. 2005: Combined sea ice thickness investigation using in situ observations, moored upward looking sonar and satellite remote sensing. *Poster, First International CryoSat 2005 Workshop, ESA-ESRIN, Frascati, Italy, March 2005.*
- Haas, C. 2004: Late-summer sea ice thickness variability in the Arctic transpolar drift 1991-2001 derived from ground-based electromagnetic sounding. *Geophysical Research Letters* 31 (L09402), doi:10.1029/2003GL019394.
- Haas, C., Gerland, S., Eicken, H. & Miller, H. 1997: Comparison of sea-ice thickness measurements under summer and winter conditions in the Arctic using a small electromagnetic induction device. *Geophysics* 62 (3), 749-757.
- Hall, R., Hughes, N. & Wadhams, P. 2002: A systematic method of obtaining ice concentration measurements from ship-based observations. *Cold Regions Science and Technology* 34, 97-102.
- Hansen, E., Løyning, T., Gerland, S. & Goodwin, H. 2004: Arctic sea ice thickness variability observed over a decade in the Fram Strait. *Extended Abstract. Arctic Climate System Study (ACSYS), 2004. Progress in Understanding the Arctic Climate System: The ACSYS Decade and Beyond. Proceedings of the ACSYS Final Science Conference, St. Petersburg, Russia, 11-14 Nov 2003. WCRP-118 (CD); WMO/TD No. 1232. September*

2004. 4 pages.

- Hvidegaard, S. M. Airborne ice altimetry methods for calibration and validation of CryoSat results. Ph D thesis, Niels Bohr Institute, University of Copenhagen and Danish National Space Center, 2005.
- Kwok, R., H. J. Zwally and D. Yi, ICESat observations of the Arctic sea ice: A first look. *Geophys. Res. Lett.* Vol 31, 2004.
- LaChapelle, E.R. 1992: Field guide to snow crystals. *International Glaciological Society, Cambridge, United Kingdom*, 101 pages.
- Laxon, S.W. "Sea Ice altimeter processing scheme at the EODC." *Int. J. Rem.Sens.* vol.15 no.4 1994.
- Laxon S., Peacock N., Smith D. – High interannual variability of sea ice thickness in thwe Arctic region – *Nature*, vol. 425, October 2003, pp. 947-950.
- Raney, R. K. and C. Leuschen: "Technical Support for the Deployment of Radar and Laser Altimeters during LaRA 2002. Final Report." John Hopkins University Applied Physics Laboratory, Maryland, USA. March 2003. Ref. SRO-03M-09.
- Romanov, I.P.: "Atlas of Ice and Snow of the Arctic Basin and Siberian Shelf Seas". Edited by A. Tunik, Backbone Publ. Comp., 277 pp., 1995.
- Sandven, S. and K. Kloster, "CryoSat Planning Document for Norwegian Pre-Launch activities". NERSC Technical Report no. 239, December 2003. CPD 2003
- Sandven, S., Alexandrov, V.Y., Gerland, S., Hall, R. & Kloster, K. 2005: Sea ice freeboard and thickness as function of snow cover and ice density. *Talk, First international CryoSat 2005 Workshop, ESA-ESRIN, Frascati, Italy, March 2005.*
- Vinje, T., Nordlund, N. & Kvambekk, Å. 1998: Monitoring ice thickness in Fram Strait. *Journal of Geophysical Research - Oceans* 103 (C5), 10437-10449.
- Vinje, T., Løyning, T.B. & Polyakov, I. 2002: Effects of melting and freezing in the Greenland Sea. *Geophysical Research Letters* 29 (23), 10.1029/2002GL015326.
- Wadhams, P., W.B. Tucker III, W.B. Krabill, R.N. Swift, J.C. Comiso, and N.R. Davis,. (1992), Relationship Between Sea Ice Freeboard and Draft in the Arctic Basin, and Implications for Ice Thickness monitoring, *J. Geophys. Res.*, 97, 20325-20334.
- Warren, S. G., I. G. Rigor, N. Untersteiner, V. F. Radionov, N. N. Bryazgin and Y. I. Alexandrov. Snow depth on Arctic Sea Ice. *Jour. Climate*, Vol. 12, pp. 1814 – 11829, 1999.
- Wingham, D. J. (ed.) "CryoSat Calibration and Validation Concept". Document CS-PL-UCL-SY-0004 of 14.Nov.2001. 96pp. (CCVC 2001)